10

Disk-Scanning Confocal Microscopy

Derek Toomre and James B. Pawley

INTRODUCTION

Rapid biological imaging of faint fluorophores in living cells — especially in four dimensions [three dimensions + time] — imposes different instrumentation challenges from slowly acquiring a single high-resolution confocal snapshot of fixed tissue. High acquisition speeds with acceptable contrast and minimal photobleaching suddenly become essential, all without losing the instantaneous optical sectioning that a confocal microscope affords. Of particular interest here, disk-scanning confocal microscopes are proving to be a powerful tool in rapid imaging of live cells in space and time. While the principle is relatively old, new instrument developments, both in optics and in novel ultra-sensitive charge-coupled device (CCD) cameras are greatly expanding the versatility and scope of this approach. However, knowing which system is best for a given question and understanding the inherent strengths and weaknesses is not easy, especially as many of the choices involve complex trade-offs between resolution, speed, sensitivity,[1] and signal-to-noise ratio (S/N). The goal of this chapter is to provide both a theoretical and a practical guide, with more emphasis on the latter especially when theoretical considerations are covered elsewhere (Chapters 22, 23, and 34, *this volume*). Here the relative merits, strengths, and weaknesses of using a disk-scanning confocal microscope for biological imaging will be examined and sample applications shown.

This chapter rests heavily on that written by G. S. Kino for the second edition, and many of his original figures and text have been retained or abridged. One notable distinction is that we have explicitly chosen to emphasize fluorescent, rather than reflected or backscattered light (BSL) imaging, as the former represents the most common use of this instrument in the biological sciences. We have also limited discussion on microscopes that are no longer in production (or are very rarely used by biologists) and instead have compared and contrasted the most prevalent current commercial disk-scanning confocal systems (Yokogawa, BD Bioscience, and Olympus) with conventional confocal light-scanning microscopy and with a new, fast confocal slit-scanning microscope from Zeiss. Finally, current limitations and new technological advances that in our opinion will markedly influence the power and popularity of this approach are discussed.

The reader is advised to pay special attention to other chapters in this volume that go into considerable depth about related subject areas: pinhole and slit detectors (Wilson and Sheppard, 1984; Wilson and Carlini, 1987; Chapters 25 and 34), signal-to-noise ratio (Chapters 22 and 23), multi-focal multi-photon microscopy (Chapter 29), photodetectors (Chapters 2 and 12), deconvolution (Chapters 23, 24, and 25), and visualization of three-dimensional (3D) datasets (Chapters 13 and 14).

BACKGROUND

Live Cell Imaging: Probing the Future

Since the publication of the second edition of this book in 1995, there has been a virtual explosion of live cell imaging papers. This is in no small part due to widespread use of genetically encoded tags, most notably green fluorescent protein (GFP) and now a literal rainbow of spectral mutants including CFP (cyan), YFP (yellow), RFP (red; monomeric and tetrameric), pH-(in)sensitive mutants, and fluorescence resonance energy transfer (FRET) probes (Miyawaki, 2003; Chapter 16, *this volume*). The immense popularity of these fluorophores derive from that fact that nearly any protein can be specifically tagged and followed in space and time. Illustrating their growing prevalence, in 1995, 2000, and 2003 there were respectively ~60, 1000, and 1600 citations of papers using "GFP." New categories of mixed chemical/genetic probes have been developed including FlAsH and ReAsH dyes which facilitate pulse-chase labeling and correlative light and electron microscopy (Gaietta *et al*., 2002). Of course, there is also a plethora of traditional vital dyes for measurements of cellular physiology (ion concentrations, membrane voltage, etc.), organelle dynamics (mitochondria, lysosomes, etc.), and fluorescently tagged ligands, lipids, and antibodies; the Molecular Probe catalogue (now Invitrogen) is an excellent reference, as are Chapters 17 and 36.[2] Very recently, small, semiconductor nanocrystals, also called "quantum dots," have been developed that are much brighter, more photostable, and have narrower emission spectra than traditional dyes (Lidke and Arndt-Jovin, 2004).[3]

What does all the progress in the probe development mean to the microscopist? As the floodgates of new specific fluorescent molecules and multi-spectral dyes have opened, there is an ever-increasing desire to **study the *dynamics* of molecules in living cells with *high spatial and temporal resolution***. The Holy Grail of such imaging is to study biochemistry at the **single molecule**

[1] Although sensitivity is a term that most people think that they understand, it lacks a specific technical meaning. We will use it here to represent a mixture of detector quantum efficiency and detector noise floor (including background). A "sensitive" detector is one suitable for discriminating a very weak light level from "black."

[2] See http://www.probes.com/.

[3] Nanocrystals have large absorption cross-sections and long decay times (τ ~10 ns). This makes them well suited for low-dose, 2-photon and confocal lifetime imaging, but can also cause singlet-state saturation at relatively low beam power.

Derek Toomre • Yale University School of Medicine, New Haven, Connecticut 06520-8002
James B. Pawley • University of Wisconsin-Madison, Madison, Wisconsin 53706

level in living cells. While this may sound like science fiction, the reality is that such scientific studies are being published using state-of-the-art probes and sophisticated microscopes (Sako and Yanagida, 2003).

A Need for Speed and Less Photobleaching

What are the **live cell** imaging needs of the biologist? There is no easy answer. Is it enough to see a single "snapshot" of a cell undergoing mitosis or is the process only revealed by time-lapse or four-dimensional (4D) imaging? Only the experimentalist can judge, but increasingly the desire to understand the complex and dynamic intra- and intercellular organization is pushing the trend towards larger multi-dimensional datasets, that include the following different spatial/temporal categories:[4]

- **2D/3D** imaging: A single two-dimenional (2D) snapshot or 3D "stack" or projection of many optical sections
- **2D + time**: Imaging of a single optical section over time. This varies from slow "**time-lapse**" (1 frame every s/min/h), to "**real-time**" (~30 frames/s), to the **ultrafast** (100–1000 frames/s).
- **4D (3D + time)**: Time-lapse (or real-time) imaging

Parameters that are generally important here are: adequate resolution (*xy*), *z*-axis optical sectioning, S/N, minimal photobleaching of fluorophores or phototoxicity to cells, and speed. How fast? This depends on the biological process being studied. For example, if studying microtubule dynamics, an acquisition of 0.1 to 1 frames per second (fps) may suffice. However, for fast processes such as calcium sparks or waves that happen in milliseconds, acquisition rates of 100 to 1000 fps may be needed.

One rule of thumb is to acquire images fast enough so that only minimal changes occur between frames (e.g., small changes in object intensity or position). In this way no action is missed and automated image analysis is facilitated. However, this "upper bound of the speed envelope" is often unrealistic, either because the imaging system cannot respond fast enough or because the sample bleaches too rapidly to obtain the desired information. This "rule" can be even more demanding when acquiring live 3D or 4D images as, in this case, each entire 3D stack must be acquired fast enough to essentially freeze the action. For example, if a vesicle is moving at 1 micron/s (a common speed) and one wishes to restrict object motion blur to ~0.25 microns, then ideally, the whole *z*-stack should be acquired in less than 250 ms. If this cell is 5 microns thick and one acquires a stack of 10 optical sections (500 nm *z*-steps), this means that each slice needs to be acquired in under 25 ms! This is not even considering the overhead time of fast (piezoelectric) focusing or the excitation of multiple dyes.

The other problem associated with 4D imaging is faster bleaching. For example, if a fluorescent sample were normally to bleach to 50% after 500 (2D) images, it would now photobleach after only 20 3D stacks of 25 planes each, or in 5 sec. if acquired at 4 stacks/s. Anyone who has attempted fluorescent time-lapse imaging, especially in 4D, knows all too well the problem of photobleaching and the proverbial proclamation that "every photon is sacred" and that 3D deconvolution reduces Poisson noise substantially by effectively averaging over ~100 voxels in Nyquist-sampled data (see Chapters 19 and 25, *this volume*).

[4] This is equally applicable for fixed cells, however, viewing living cells avoids fixation artifacts and can facilitate rapid screening of samples (e.g., GFP-based visual screens).

Advantages and Limitations of Confocal Laser-Scanning Microscopes

Why are confocal laser-scanning microscopes (LSM), so popular with the biological community in spite of their quarter to half million dollar expense? The single major advantage of the confocal LSM is the ability of its **spatial filter** (either a single pinhole or a slit) to reject out-of-focus light. This improves contrast-reducing background or haze, and provides better optical sectioning (and resolution) along the *z*-axis, although a ~30% increase in lateral (*xy*) resolution is possible if the pinhole is closed to about 0.05 Airy units[5] (Wilson and Sheppard, 1984). Given the many attributes of this mature technology, why should one use any other kind of light microscope for fluorescent imaging?

Alas, the source of its strength, the single confocal pinhole, is also its Achilles' heel, creating problems that while of little concern with bright, fixed cells, can be disadvantageous for fast or long-term imaging of living cells.[6] Let us start by considering the data rate. As is clearly demonstrated in Figure 35.19 (Chapter 35, *this volume*), the most important factor in obtaining a good, high-contrast image is to collect enough photons! Otherwise statistical noise in the signal makes the image grainy and smaller features become invisible. This means that both the collection of light (lens and intermediate optics) and its detection must be optimal. Most confocal LSM use **photomultiplier tubes (PMTs)** for detecting photons. Although they have a rapid response and good dynamic range, their **effective quantum efficiency (QE)** is low, typically only in the 6% to 15% range (in the 400–600 nm spectrum). This stands in stark contrast with the up to 90% QE achievable with a good back-illuminated, CCD camera (see Chapter 13, *this volume*).

Because the rate at which data can be derived from a fluorescent specimen depends directly on the number of excitation photons striking it, to image at the same frame rate, the intensity of the light in the single spot of an LSM must be about ~10^5 times higher than that used in a widefield (WF) system. This very intense excitation light can lead to **dye saturation** (see Chapters 2 and 16, *this volume*), a phenomenon that occurs when the excitation is so bright that most of the dye molecules are in the excited state. Using more laser power only raises the background because, as molecules away from the focus plane are now excited more strongly, but are still not saturated, they will produce relatively more out-of-focus light. It also increases photobleaching without increasing signal level (Chapters 38 and 39, *this volume*, discuss the relationship between bleaching and saturation). Saturation can only be minimized by using a dye with a faster singlet decay time or by using less intense light.

On the other hand, rapid fluorescent imaging requires more intense light so as to produce a similar number of emitted photons in a shorter time.[7] Clearly there is a theoretical maximum imaging speed set by the total **rate at which photons are generated**

[5] Rarely is this done when viewing live biological samples as signal level decreases approximately with the square of the pinhole diameter and low signal is much more a barrier than simple optics to seeing even the Abbe resolution.

[6] Note that when commercial single-beam confocal microscopes first appeared two decades ago, living cell fluorescent imaging was uncommon and a premium was put first on the optimization of resolution and later on multi-spectral excitation and detection, rather than on speed or sensitivity. Paradoxically, Zeiss' 2004 release of their LSM 510 LIVE confocal is based on a lower resolution slit scanner.

[7] An analogy can be drawn to filling up buckets with water, either drip-by-drip over hours or in a second with a fire hose.

(depending on the number of beams, the excitation intensity in each one, and the photoproperties and concentration of the dye) and the **photon efficiency** of the entire detector channel. Although one can increase signal level by using more dye, this can seldom be done without affecting functionality; for example, protein overexpression can cause misfolding or mislocalization.

One alternative is to scan a very small area of interest or even just a single line to gain frame speed. However, when sampling only a small region, information on a larger spatial scale is lost.[8] In fact, **weakly labeled samples are triple hit**; more intense light is needed to excite the dye to generate enough photons, leading to more background, phototoxicty, and increased photobleaching.

The second requirement for fast confocal imaging is that both the laser beam and the image of the pinhole must be raster-scanned over the sample — typically using linear galvanometers. The **mechanical properties of** linear galvanometers limit how fast a line can be scanned (low kilohertz, see Chapter 3, *this volume*). Although acousto-optical deflectors or resonant galvanometers can go faster, they have their own limitations (see Chapter 9, *this volume*). Finally, lasers are expensive and by definition only excite at very discrete "lines," limiting the fluorescent dyes that can be excited.

Other Imaging and Deconvolution

Is confocal imaging the only way to go? As mentioned above, the advantage of a (1-photon) confocal is to reduce background by rejecting out-of-focus **emission** light with a pinhole. Alternatively, one can make optical section images by limiting the **excitation** to a single optical plane or by using other microscopical techniques, for example, 2-photon excitation (Chapters 28, 29, and 37, *this volume*) or total internal reflection fluorescent microscopy (Toomre and Manstein, 2001). When imaging samples in which most or all of the dye is confined to a single optical plane (e.g., some *in vitro* assays), widefield (WF) epi-fluorescent imaging may suffice.

Alternatively, one may acquire a stack of WF epifluorescent images and use a measured, or theoretical, point spread function (PSF) to "deconvolve" the 3D image. The principle here is that at least some of the out-of-focus haze can be converted into useful information. While a detailed analysis of deconvolution is provided in Chapters 23 and 24, it is worth underscoring the following limitations of deconvolution:

- Deconvolution is time consuming (especially for 4D datasets) and does not give on-the-fly results.
- Small misalignment of the optics can prevent good deconvolution.

The quality of the deconvolution depends on the sample and the method of deconvolution (there are several). However, there is also some good news: deconvolution will also improve the image quality of confocal 3D datasets by suppressing out-of-bandwidth "features" caused by Poisson noise and effectively averaging signal levels over many voxels. In addition, because the confocal PSF is confined to a much smaller volume, the computer processing time is greatly reduced.

[8] Often one only determines *a posteriori* what region of an image was important.

CONFOCAL DISK-SCANNING MICROSCOPY

Nipkow Disk — An Innovation

The **Nipkow disk** that is central to the design of all modern disk-scanning confocal microscopes, was developed by Paul Nipkow in 1884 as a means of dissecting an image into a single continuous signal. Nipkow had the foresight to realize that if a series of pinholes (or squares) were arranged in an Archimedian spiral of constant pitch, then one revolution of the disk would be equivalent to scanning the object (see Fig. 1.3, *this volume*) and the light transmitted by the holes could be measured to record any image projected onto the disk. It was an early competitor of the television we know today. Apart from its mechanical complexity, its main weakness was that at any given time light is only detected (or transmitted) through a single small pinhole making it inefficient for detecting or displaying image information. This is why televisions no longer use Nipkow disks.

More recently, Petráň designed a new a new type of Nipkow disk, one having many more holes arranged in a series of nested spirals so that hundreds or thousands were present in the frame at any one time and in such a way that the entire pattern was axially symmetrical (Fig. 10.1).

A Renaissance — Advantages of Disk-Scanning Confocal Imaging

Disk-scanning imaging was reborn in 1967 in Egger and Petráň's first implementation of a **tandem scanning-disk confocal microscope**. The purpose of the Petráň disk was not to dissect the image (as in Nipkow's design) but to perform point-illumination/point-detection confocal imaging. Light transmission through a Petráň disk is hundreds to thousands of times higher than through a Nipkow disk.[9] New designs by both individuals (e.g., Kino, Xiao,

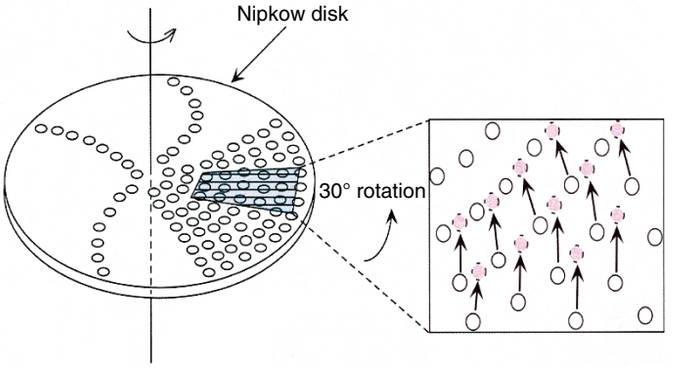

FIGURE 10.1. Schematic of a Nipkow/Petráň disk used in real-time disk-scanning confocal microscopy. Typically 20,000 to 200,000 pinholes are arranged in spirals of constant pitch (Archimedian) and a subregion (shown in blue) corresponding to about a thousand pinholes are illuminated and imaged. A partial rotation (e.g., 30° for the Yokogawa CSU10/22) of a rapidly disk-scanning (~1800–5000 rpm) scans the sample; arrows show how holes rotate to new positions (red). Images can be seen in real-time by eye or acquired using a camera that is synced with rotation of the disk. (Image adapted from H. Ishida *et al*., Department of Physiology, Tokai University.)

[9] Note on nomenclature: many people and companies call spinning confocal disks "Nipkow disks" even though the pinhole spacing and design may be radically different from the original Nipkow disk. Thus, a "Nipkow disk" merely denotes a **spinning disk** pinhole- (or slit-) based confocal system rather than a specific design.

TABLE 10.1. Comparison of Confocal LSM, Disk-Scanning, and Scanned Slit Microscopes

	Single-Beam Laser Scanning	Spinning Disk	Scanned Slit
Advantages	• High resolution • Excellent, adjustable *z*-resolution • FRAP/photoactivation • Simultaneous readout of several wavelength channels	• High speed • Good QE detector and sensitivity • Moderate cost[a] • Laser not required	• High speed • Good QE detector and sensitivity • Simultaneous readout of several wavelength channels
Disadvantages	• High cost • Slow to moderate speed • Low QE detector • High excitation intensity • More photobleaching • Requires lasers	• Lower resolution and *z*-resolution[b] • Fixed pinhole/slit • Low transmission of excitation[c]	• Lower resolution and *z*-resolution • Requires lasers • High cost • No FRAP

[a] Large price range from ~US$35,000 to US$300,000 (see Table 10.2).
[b] Depends on the pinhole/slit setting (see text and Fig. 10.4) and operationally on the light budget.
[c] An exception is the Yokogawa microlens design, which transmits more excitation light.

Boyde, Lichtman) and companies have further expanded the possibilities, however all disk scanners share common features. The optimal pinhole (or slit) size and spacing is important and will be discussed later and in Chapter 11.

The disk is located in a conjugate image plane and a partial rotation of the disk scans (see arrows) the specimen with thousands of beams of light that can cover the whole image plane in as little as 1 ms. While a single-beam confocal LSM illuminates and collects intensity information **serially**, multiple pinholes allow the specimen to be sampled in **parallel**. This produces a **multiplicative gain in potential scan speed** proportional to the number of pinholes present in the illumination/detection system.

As the Petráň microscope requires the illumination of a wide-field of pinholes, rather than a single small spot, a conventional "white" light source such as a mercury or xenon lamp can be used instead of a laser. Disk scanning is more rapid than the human visual flicker response rate (~18 Hz) and a **"real" confocal image** of the sample can be seen by eye or detected with a camera in true color.

Some of the earliest applications of disk-scanning confocal microscopes (e.g., Petráň, Kino, and colleagues) were to illuminate the sample with white light through the pinholes and collect light reflected from the confocal plane. When such a system employs objective lenses intentionally designed to have very high chromatic aberration, light of different wavelengths forms foci at different heights. The result is that images of opaque, reflective specimens are colored with each color representing features of a particular topographic elevation. By inserting diffraction gratings into the eyepieces of the microscope, such images can even be viewed as real-time stereo-pair images. As the gratings displace the location of features horizontally depending on their color, and as their color is coded for depth by orienting the gratings in opposite directions for each eye, a stereo-pair image is presented in which the actual 3D position of the specimen surface is both coded by color and made visible by stereo disparity (Chapter 15, *second edition*).

Advantages of disk-scanning include:

- **Up to 100- to 1000-fold gain of speed**: multiple points of light illuminate the sample and are detected **in parallel**, greatly reducing fluorophore saturation.
- Generating a **real image** that can be detected by eye or with a fast, high-QE CCD camera.
- **Less photobleaching** (due to lower local excitation intensity).
- **No** strict requirement for **laser** illumination, reducing cost and allowing more choices of excitation wavelengths.

Disadvantages

Several factors must be considered when using a disk-scanning confocal (see Table 10.1). First, light scattered or fluoresced by structures away from the focus plane can still reach the detector through an adjacent pinhole, decreasing the *z*-resolution of the system. Second, low transmission of light through the disk may hinder imaging of dim fluorescent samples. Although this can be compensated with longer exposure times, doing so negates the speed advantages that are sought. However, a high-QE detector may still give slow confocal imaging with less bleaching than a confocal LSM. Third, 90% to 99% of illumination light does not go through the disk and these reflections can cause high background, especially in single-sided bright-field spinning confocal microscopes. Field illumination may not be uniform and may require a correction lens and/or homogenization of the arc source (e.g., a liquid light guide). Finally, disk-scanning systems do not allow high power illumination of selected regions of interest for fluorescent recovery after photobleaching (FRAP) experiments. These disadvantages can be partially mitigated by judicious choice of intermediate optics, pinhole or slit size and spacing, detector type, and the addition of a separate bleaching system.

CRITICAL PARAMETERS IN PINHOLE AND SLIT DISKS

Fill Factor and Spacing Interval F

Although the present discussion has centered on confocal pinholes, the use of a confocal scanning disk with slit apertures can increase the transmitted light budget. Slits can either be arranged on the disk as spirals or in linear arrays. The main **trade-off between slit versus pinhole** is usually between **brighter illumination and higher signal with a slit design and better *z*-resolution with pinholes**. Slit-disk confocals have a larger percentage transmission (T), or fill factor, than pinholes when the ratio of the slit/pinhole diameter, D, to distance between slits/pinholes, S, is fixed:

$$T_{\text{slit}} = \left(\frac{D}{S}\right) \times 100 \qquad T_{\text{pinhole}} = \left(\frac{D}{S}\right)^2 \times 100 \qquad \textbf{(1)}$$

For example, if $D = 50$ microns and $S = 500$ microns, then 10% and 1% of the light will be transmitted by a disk with slits, and pinholes, respectively. The transmission of the pinhole disk can be increased by using a smaller pinhole spacing interval. However,

even if *D*/*S* is 1/5, only 4% of the light will be transmitted, and smaller *D* causes too much of the emitted light to return through neighboring pinholes, decreasing *z*-resolution,[10] as discussed below.

Other options are to increase the pinhole or slit diameter, however, this will decrease the axial resolution (see below). Alternatively, intermediate optics employing "microlenses," such as those used in the Yokogawa system, can focus more of the excitation light onto the pinholes but only if laser light is used. It is worth noting that when the slits are very close, this imaging system begins to resemble structured illumination (e.g., Zeiss Apo-tome; see Chapter 13, *this volume*) although there, signal detection is ***not*** confocal.

Lateral Resolution

The *xy*-resolution of the light microscope is described by the Abbe equation and is a function of the emission wavelength and numerical aperture of the objective:

$$r_{\text{Airy}} = 0.61\frac{\lambda_o}{NA_{\text{obj}}} \quad \textbf{(2)}$$

In biological fluorescence confocal microscopy, where overall performance drops rapidly because of poor signal statistics if *D* is reduced below one Airy unit, *xy*-resolution is essentially the same as that of the widefield instrument. This is particularly true for disk scanners having *D* that is more than 2 Airy units because, in this case, the CCD will record a mini-image from the light returning through each pinhole.[11]

Pinhole/Slit Size

What is the optimal pinhole size? Unlike confocal LSMs, which offer a diffraction-limited spot as the excitation pinhole and separate independently adjustable pinholes for each detection channel, disk-scanning confocals use the same pinhole for excitation and detection (or in tandem systems, one of identical size). While in both types of confocal, increasing *D* increases signal strength because light can now reach the detector from features farther from the focus plan, only in disk scanners does it also produce more signal because there is more excitation light striking the specimen in the larger excitation spot. This makes pinhole size important.

The **optimal diameter of a pinhole/slit**, D_{OPT}, sets it equal to the FWHM of the Airy figure and can be derived from the Fraunhofer formula (Goodman, 1968; Kino, 1987; Kino and Xiao, 1990) and expressed as the following approximate equation;[12]

$$D_{\text{opt}} = \frac{0.5\lambda h_1}{b} = \frac{0.5\lambda M}{NA} \quad \textbf{(4)}$$

where *M* and *NA* are, respectively, the magnification and numerical aperture of the objective lens. Assuming a 100× 1.4 NA oil-immersion lens, and λ = 560 nm, D_{OPT} is 20 µm but only 9.3 µm for a 40× 1.2 NA lens. Thus, one needs disks with different *D* values for objective lenses with different *M*/*NA* ratios. In commercial systems with a single disk (Yokogawa and CARV), the pinhole was designed for high magnification, high NA objectives, and even then the 50 to 70 micron pinhole diameter is excessively wide (Table 10.2).

The effects of pinholes (or slits) that are the wrong size are shown schematically in Figure 10.2. A small pinhole has decreased transmission due to its small area and also, because the illumination light diffracts at the aperture, the light from it overfills the pupil of the objective lens, wasting more light. On the detection side, an **overly small pinhole** rejects more light than necessary and decreases the S/N (identical to when one closes the pinhole too much in a confocal LSM). Alternatively, if the **pinhole is too big** then and the (non-laser) illumination is collimated rather than convergent, then it may not be diffracted adequately to fill the pupil of the objective, illuminating a larger spot at the focus plane.[13] Signal light from this larger spot will be imaged as a mini-image in the aperture of the disk. The emitted light is collected efficiently but the large pinhole makes the *z*-resolution worse. Some commercial systems allow one to change the slits to match the objective (DSU unit) while in others the pinholes are fixed (Yokogawa CSU series and CARV) and only the magnification of the objective or the tube can be adjusted to change the effective size of *D*.

Use of the ***same*** **pinhole or slit for both illumination and detection** causes the *z*-resolution of the non-laser disk-scanning confocals to fall off much more rapidly as *D* increases than occurs with single-beam confocals.[14] However, when the ***D*** **is optimal**, the curves for the single- and multi-beam scanners converge, as long as one ignores haze reaching the CCD through adjacent pinholes.

Axial Resolution

The **axial resolution**, *dz*, near the focal plane of slit and point scan confocal microscopes with very small pinhole/slit dimensions can be expressed by the equation

$$d = K\frac{\lambda}{n\left[1-\sqrt{1-\left(\frac{NA_z}{n}\right)^2}\right]} \quad \textbf{(3)}$$

where λ is the emission wavelength, *n* is the refractive index of the medium, *NA* is $n \sin\alpha$ (α is the acceptance angle of the objective of), and *K* is a scalar correction factor where for a slit disk K_{slit} = 0.95 and for a pinhole disk K_{pinhole} = 0.67. For example, if λ = 500 nm, NA = 1.2, and *n* = 1.33 then *d* would be 627 nm and 442 nm for a slit disk and pinhole disk, respectively. As long as *D* is the same for both pinholes and slits and also significantly smaller than the calculated Airy limit, slits will have ~1.4× worse optical sectioning than pinholes.

However, this statement really does not tell the whole story. If one were to make a *z*-scan through a thin, horizontal layer of dye,

[10] Also applies to slits (see graph in Fig. 10.9).

[11] This mini-image will have dimensions only a few pixels in size and the information it contains can only be recorded as long as the magnification of the camera lens is sufficient to match these pixels with the size of the pixels on the CCD.

[12] This sets the pinhole diameter at the full-width half-maximum of the Airy figure and lets through about 75% of the light in the central maximum. In biology, the pinhole/slit is often set at the first zero of the Airy figure, about twice as big.

[13] In laser-illuminated disk scanners, the high coherence of the source insures that the light is focused into an Airy figure no matter what the size of the aperture. However, the size of this figure depends on the extent to which light from each aperture fills the back-focal plane (BFP) of the objective, a factor that can be increased by the convergence angle of the light striking the disk.

[14] In laser-illuminated disk scanners, assuming that the divergence of the light leaving each pinhole is sufficient to fill the BFP of the objective, each excitation beamlet is focused into a single, diffraction-limited spot, regardless of the pinhole size. This occurs because of the extremely high coherence of laser light.

TABLE 10.2. Comparison of Some Different Microscope Specifications[a]

				Disk-Scanning Confocal		
Microscope Parameters	Epi-fluorescence	Confocal Point LSM	Confocal Line LSM	Yokogawa (CSU10/22)	CARV[b]	DSU
Supplier/Distributor	All major manufactures	Many: Zeiss, Leica, Olympus, Nikon . . .	Zeiss (LSM510 Live)	(Yokogawa) / PerkinElmer, Solamere Tech. McBain Instruments, Visitec[c]	Atto Bioscience	Olympus
Scan Type	No	Point scan	Line scan	Disk	Disk	Disk
Pinhole/Slit	None	Pinhole or slit	Slit	Microlens + pinhole	Pinhole	Slit
Adjustable pinhole/slit	n/a	Yes	Yes	No	No	Yes
Illumination	Hg or xenon arc lamp	Laser(s)	Lasers (diode)	Laser(s)	Hg or xenon arc lamp	Hg or xenon arc lamp
UV excitation	Yes	Yes, but need expensive laser	Yes (405 nm)	Only specified for 400–650 nm	Yes[d]	Yes
Pinhole or slit size/spacing diameter (μm)	n/a	Adjustable pinhole or slit	Adjustable slit	Pinhole 50/250	Pinhole 70/~250	Slits 13–38/140–400
Disk fill factor	n/a	n/a	n/a	4%	5%–7%	5%–10%
% Transmission pinhole/slit	~100%	~50%	> 90%	~40% with microlens	~5%–7%	5%–10%
Detector	CCD	PMT	Linear CCD	(EM) CCD	(EM) CCD	(EM) CCD
Detector: Max QE[e]	~50%–90%	~10%–20%	~50%–80%	~50%–90%	~50%–90%	~50%–90%
Full image scan rate[g]	n/a (no scan)	~1 fps (faster for ROI)	~120 fps @ 512 × 512	1000 fps	200 fps	~50 fps
Max. z-resolution	(Very poor)	Best	Moderate	Good	Good	Moderate
Cost	Inexpensive	Expensive ($200 K–$400 K)	Expensive (TBA)	Expensive ($100 K–$300 K)	~$50 K	~$35 K
Microscope compatibility	N/A	Usually sold with microscope	Zeiss	Many: inverted or upright	Many: inverted only	Olympus: inverted or upright
Relative space requirements	Small	Variable: medium/large	Medium	Large including laser	Medium	Small
Filter options; Exchangeable?	Standard; yes	Many internal filter options; no	Many internal filter options; no	1–3 filter cubes[f]	3 filter cubes; yes	6 filter cubes; yes

[a] Not an exclusive list and parameters may change.
[b] A CARV2 instrument will have 5× faster scanning and FRAP capacity.
[c] Supplied by Yokogawa (Japan) and distributed by PerkinElmer as part of the Ultraview microscope, Solamere Technology Group, McBain and Visitec as stand-alone or integrated units with lasers, integration software, etc.
[d] Post-disk intermediate optics do not transmit well in the lower UV (cutoff ~370 nm).
[e] Depend on camera/PMT model and spectral response curve (e.g., see Fig. 10.8).
[f] Acquisition speed may be limited by camera speed and/or number of photons collected. Note: When a line is scanned only once (maximum speed), it is possible that information may be lost or duplicated unless sychronization between disk position and camera exposure time is perfect.

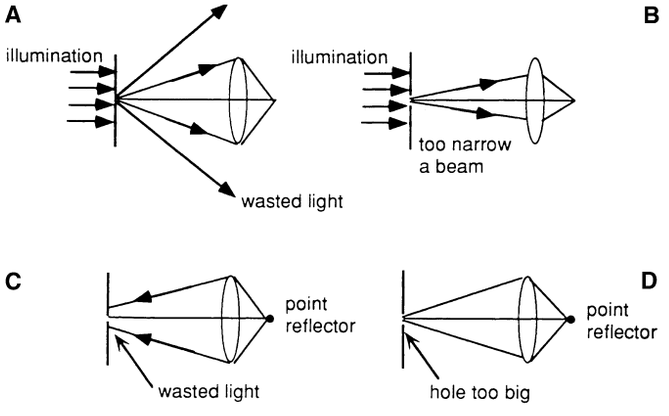

FIGURE 10.2. Ray paths with different pinhole sizes. (A) Pinhole too small wastes transmitted light with too wide a beam. (B) Pinhole too big yields a narrow beam and low effective aperture. (C) Pinhole too small wastes received light. (D) Pinhole too large gives poor definition.

there would be a peak as the focus plane coincided with the dye layer and Eq. 3 would describe the width of this peak. However, this peak would have a very long tail because an amount of light about equal to the square of the gross transmission of the disk would still reach the CCD through the wrong pinhole, even when the dye layer was very far out of focus. It is this tail of diffuse background haze that will limit overall performance whenever one observes specimens that are both thick and heavily stained and the amount of this background is proportional to the transmission of the disk.

Therefore, while Eq. 3 may provide a good estimate of the accuracy with which one can determine the surface height of a highly reflective semiconductor using a disk scanner with small pinholes placed on a sparse grid and a dry objective of relatively low NA, it fails to account for the many important practical matters that affect fluorescence imaging in transparent specimens. As the signal reflected from a semiconductor can easily be $10^5\times$ higher than that produced by a fluorescent specimen, D can be much less than one Airy unit. In addition, as the height variations of the semiconductor are both known and fairly small, it is possible to choose S large enough so that little light reflected from, for example, the highest feature, is sufficiently out of focus to pass through neighboring pinholes when the focus plane coincides with the lowest feature. Last but not least, as the structures of semiconductors tend to be relatively horizontal and opaque, one is usually more interested in determining the location of the outer surface (z-position, the height of peak reflection) than trying to see one feature below another (z-resolution).

However, in biological disk-scanning where the NA is high, the specimens are transparent and the signal levels are so low that D/S >0.1, the fact that Eq. 3 takes no account of light coming through the wrong pinholes is a serious limitation. Let us call this light WP light (for wrong pinhole).

Clearly, the amount of WP light that reaches the detector depends on the staining pattern in the specimen. If the stain is confined to a horizontal plane that is thin in the manner defined above for a semiconductor, then there is little problem. However, because D and NA are now larger and S is smaller, the band of z-heights for which this is true is thinner. As the exact manner in which this plays out is both important to understand if one is to appreciate the optical sectioning properties of disk scanners and is also poorly conveyed by equations, we will attempt a more heuristic explanation.

Figure 10.3(A) shows a red fluorescent point object emitting light in all directions. We will not yet discuss how it is being excited except to note that the process follows exactly the same rules as are described below, except in reverse. Only some of the light leaving the point hits an objective lens having an acceptance half-angle of 45° (e.g., an NA 1.0 lens). The broken black horizontal line represents a disk with pinholes in it. Although the actual disk is located in the intermediate image plane on the other side of the objective, we can see its masking effect just as well in any image plane, including the focus plane in the specimen as shown here. In fact, it is rather instructive to imagine that the pinhole is sampling the light field near the focus plane.

In Figure 10.3(A), the point object is seen lying in the focus plane and, as we have assumed that D is 1 Airy unit in diameter (i.e., ~0.5 µm, when referred to the focus plane), and that essentially all of the light from the central maximum of the Airy disk that represents the point object goes through the pinhole and proceeds (via optics that are not shown) to the CCD. Figure 3(B) shows the layout of the disk viewed *en face*. The D/S is about 1/5, implying a S spacing of about 2.5 µm and a total transmission of ~4%, about normal for many disk scanners used in biology.

When the stage moves down, the point object drops below the focus plane, and the amount of light going through the central pinhole in the disk drops [Fig. 10.3(C)] because the light leaving the point object at any angle that the objective can accept now mostly strikes the bottom of the disk, as is represented by the pink disk in Figure 10.3(D).

When the point object is 2.5 µm from the focus plane of the NA 1 objective, the defocus equals S and some of the light from the point begins to pass through the first ring of neighboring pinholes, but not very much. In simple terms, 6× more light will now reach a CCD pixel that is focused on the wrong pinhole than reaches it through the proper pinhole. However, the light from the object that, at focus, was concentrated into a spot 0.5 µm in diameter is now spread over one with five times the diameter and 25× the area and, as the same diminution in intensity is occurring on the excitation side, the number of fluorescent photons/square centimeter at the plane of the disk is now 625× lower than it was at focus. As the pinholes are laid out as equilateral triangles, one can see from Figure 10.3(B) that only about D/S of the light striking the annulus with radius S and thickness D actually passes through the disk. This fraction would be much higher were we referring to an array of parallel slits.

As the point moves farther out of focus, the absolute number of photons reaching the CCD from the point continues to diminish until some light starts going through the ring of second neighbors, about 4 to 5 µm away from the focus plane.

We can see from Figure 10.3 that if the NA is higher, this same process will occur at lower defocus values, and vice versa.

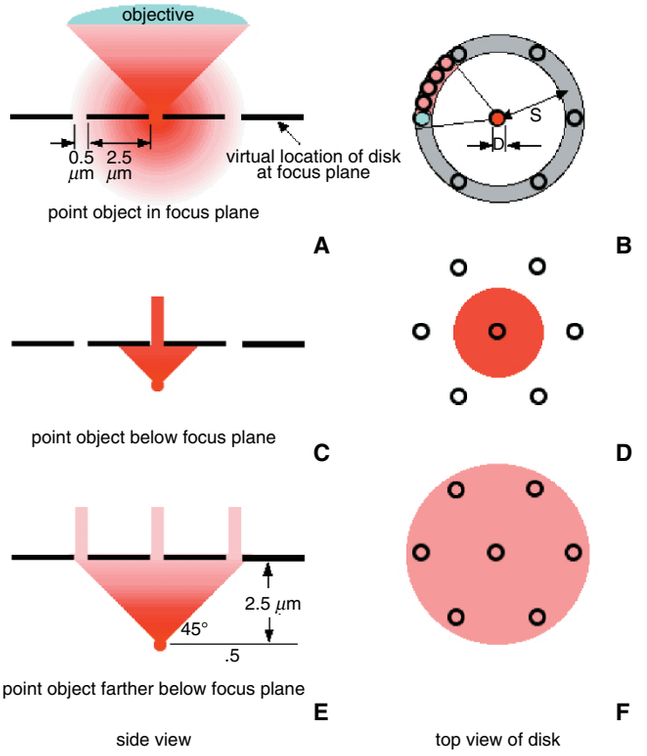

FIGURE 10.3. Diagrams showing how light originating from out-of-focus planes passes through adjoining pinholes to create a haze level and how this process is affected by the geometry of the pattern of the holes in the disk and the convergence angle of the objective, as described in the text.

So far so good. But what if instead of having a point object, we have an unpoint, a black hole in a sea of dye. When the unpoint is in the focus plane, a pinhole that should measure zero will not do so because other beams will be exciting dye above and below the specimen and some of this light will be out-of-focus enough to come through the pinhole that should be dark. Long before the dark point is distance S from focus, it will become invisible. The geometry that helped reduce the brightness of the out-of-focus point object by 625× no longer works because, beyond a defocus of $\pm D$, the diminution in intensity that occurs as the diameter of the cone of light from a single point is supplemented by brightness from the now-overlapping cones of fluorescent light from nearby holes.

Although Figure 10.3 discusses round apertures, similar reasoning can be applied to linear ones, with the exception that, when the defocus equals D, a larger fraction of the light will go through the next slit than went through the six nearest pinholes. This fact is often taken as evidence that "slit-scanners do a worse job of optical sectioning than point-scanners." However, if we keep the transmission of the two disks the same, the D/S of a slit disk will be smaller and, assuming that we choose the same D value based on the resolution of the objective, S will be larger and in the final situation stray light situation will be much the same as with pinholes. Yes, a greater fraction of the light goes through the next slit but now this will not happen until the defocus is greater and, consequently, the light intensity in photons/square centimeter, is lower. Indeed, as a slit scanner with a larger S value has a deeper band of z-values for which no overlap occurs, it could be said to provide better optical sectioning.

Clearly, any curves plotting the z-resolution of disk scanners inherently include assumptions about the stain distribution in the specimen, not only its thickness and pattern, but in the case of some line scanners, also its orientation in the xy-plane. In other words, any simple statements regarding the optical sectioning abilities of disk scanners that fail to discuss the nature of the specimen do not convey much useful information to the biologist.

Figure 10.3 shows that

- For specimens in which stained structures are confined to a thin layer, or for thicker specimens in which the stain is concentrated in clumps that represents only a small minority (say <1%) of voxels, disk scanners can approach the optical sectioning performance of single-beam confocals.
- Choosing a larger S increases the zone of best sectioning performance but also reduces signal levels.
- Specimens composed of heavily stained structures that extend over a range of depths will pose more problems.
- In the final analysis, optical sectioning performance has more to do with the transmission of the disk than with whether the apertures are slits or pinholes.

As will be discussed below in the section on electron multiplying CCD (EM-CCD), it is significant that all geometries will permit more light from objects that are far from the focus plane to reach the detector than would be the case with single-beam scanners.

TYPES OF DISK-SCANNING CONFOCALS

General Considerations

In disk-scanning microscopes, the scanning disk is positioned in an image plane. For all systems, but especially for those using reflected or backscattered light, it is important to prevent excitation light from reflecting off the disk and reaching the detector. Although most of the 90% to 99% of the light that does not pass through the disk (except the Yokogawa design) is absorbed by it, the amount reflected from even the blackest surface is immense compared with that returning from the specimen. This reflected light can be eliminated using barrier filters as long as the system is used to detect a fluorescent signal but other techniques must be used when the microscope is used to collect backscattered or reflected light. The disk-scanning units are often attached to the side port (camera) or back port (lamp) of the microscope and either a mercury/xenon arc lamp or laser fiber-optic (Yokogawa) is attached to the unit. A detailed comparison of the hardware specifications of common, commercial, epi-fluorescent, confocal LSM and disk-scanning microscopes is shown in Table 10.2.

Disk Scanners for Backscattered Light Imaging

The Tandem-Scanning Confocal Microscope

The earliest design of a disk-scanning confocal microscope used a tandem pinhole design (Petráň *et al*., 1968, 1985) in which pinholes arranged on the disk in a symmetric pattern of interleaved right- and left-handed Archimedian spirals, illumination and detection occur in tandem, through separate pinholes on opposite sides of the disk. The illumination entering one pinhole goes through the objective, and light reflected from the sample is optically rerouted via a set of mirrors and a pellicle beam-splitter to a second set of conjugate pinholes located on a diametrically opposed spiral (see Fig. 10.4). This convoluted light path was used to prevent glare reflected from the disk from reaching the ocular. This was a

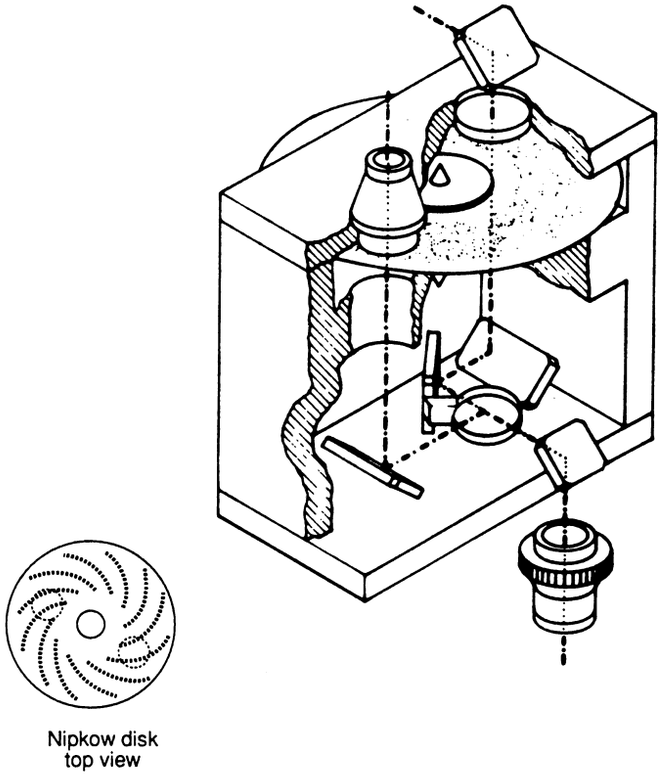

FIGURE 10.4. The tandem scanning reflected light microscope (Petráň *et al*., 1985).

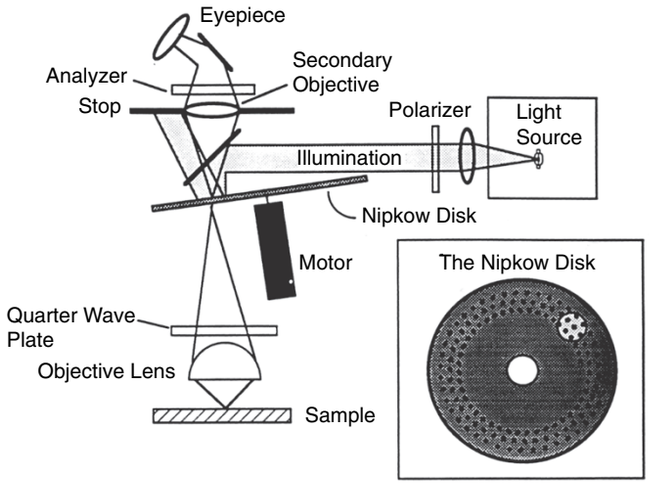

FIGURE 10.5. The single-sided scanning confocal light microscope (Xiao and Kino, 1990).

tremendous advantage when looking for weak backscattered-light signals but the difficulty of making and orienting a dichroic mirror on the surface of the pellicle beam-splitter made this design difficult to use for fluorescence. Not only was it hard to change the beam-splitter without ruining the alignment, but the intensity was so low that one still needed to make long exposures, thereby negating the advantages of the high scan speed. The other major limitation of this microscope was its mechanical complexity and the difficulty of properly translating the mirrors in three dimensions and tilting them along two axes. In fact, scan lines were always visible. A commercial version of this microscope using 40 to 70 micron square pinholes was produced by Noran (now Thermo-Noran, Middleton, WI, model TSM, now discontinued).

Single-Sided Disk Scanning Confocal Microscope

The single-sided disk-scanning confocal microscope designed by Gordon Kino (Xiao and Kino, 1987; Xiao *et al*., 1988; Lichtman *et al*., 1989) uses the same set of pinholes for illumination and detection (Fig. 10.5). It has a simple optical path that incorporates a number of features to minimize glare from the disk. The holes are etched in a polished black chrome coating evaporated onto a quartz disk and this disk is placed in the intermediate image plane at a slight angle so that excitation light is reflected off the optical axis to where it can be trapped by a beam stop. For BSL imaging, the input light is polarized and after being transmitted through the disk it passes through a quarter wave plate in front of the objective lens so as to produce circularly polarized light. Light reflected by the specimen undergoes the reverse effect and an analyzer placed in front of the eyepiece/camera selects against light reflected from the disk and passes light reflected from the specimen.

The disk on Kino's microscope contained ~200,000 pinholes of 25 micron diameter and spun at ~2000 rpm, giving a scanning speed of up to 700 frames/s. As the pinhole is near the optimal diameter for use with a high magnification, high NA lens, the resolving power of this system is similar to that of a single-beam confocal LSM, but much faster! Köhler illumination (Born and Wolf, 1998) is used so that standard epi-fluorescent (or bright-field) imaging can be achieved by removal of the disk. Important optimization parameters include adjusting the mercury (or xenon) arc so that illumination is uniform over the field of view. An aperture stop limits stray light and a field lens, positioned below the disk, decreases vignetting. For fluorescent imaging the 50/50 beam-splitter can be replaced by an appropriate fluorescent filter cube, as in epi-fluorescent microscopy.

Disk Scanner Designs for Use in Fluorescence

Because of its simplicity, the single-sided disk scanner is by far the most popular style of confocal disk-scanning microscope. Tricks such as tilting of the disk and the use of anti-flex techniques are unnecessary because modern dichroics and barrier filters can prevent almost all excitation light from reaching the CCD. Several commercial systems suitable for fluorescent imaging use variations of this design.

CARV, DSU, and Other Disk-Scanning Confocal Microscopes

Early commercial, fluorescent, single-sided disk systems were sold by Technical Instruments system (K2-Bio) and Newport Systems (VX100 confocal adaptor).[15] In the former, the upper part of a standard microscope was replaced with the disk and illumination system. The later system is based on an instrument developed by Jeff Lichtman (Lichtman *et al.*, 1989) and was sold as an attachment for an upright microscope. Briefly, a 4× low NA lens is used to image the disk scanner, mounted on a secondary external stage, onto the CCD. The secondary stage contains compact intermediate optics and a high NA main objective is used to image the specimen onto the disk. In both systems, the disk had separate tracks with different sized pinholes or slits so as to match the magnification of the objective or light budget of the application, but only the KCS Bio used normal, highly corrected microscope objectives under optimal optical conditions. The CARV (Boston, MA; Fig. 10.6; Table 10.2) uses a mercury arc lamp for excitation and mounts onto the left-side port of an inverted microscope. It uses 60 µm diameter pinholes at ~250 µm spacing, scans at 200 fps, and has ~5% to 8% transmission. As these pinholes are well above the Airy limit of even the highest magnification lens, *z*-resolution is moderate even when one utilizes the 1.5× auxiliary magnifier now found on some microscope stands to change a 100× objective into one with 150×. The user can see the live, confocal image through a second binocular head, but this system is relatively bulky and does not work with upright microscopes. The CARV2 with a faster scanning speed (1000 fps), automated filters, and the ability to do **FRAP** by switching the Nipkow disk with a photobleaching slit, has just been introduced.

A new disk-scanning unit, the **DSU** by Olympus (Figs. 10.7 and 10.8; Table 10.2) uses a **multi-slit** design in which half the slits are horizontal and the other half are vertical on the disk. The user can switch between five **different disks** (DSU1–5) each having a different fill factor (5% to 10%) and slit width (13 to 38 µm) for use with both low and high magnification objectives. The confocal head is compact, but as it attaches to the back Hg lamp port of either inverted or upright Olympus microscopes, direct viewing through the eyepiece is not possible. It has an adjustable field stop and, as the intermediate optics are part of the conventional illumination path, it is fully UV compatible. As shown in Figure 10.8 (bottom), $S > 8S$ (12.5% fill factor), otherwise the resolving power decreases substantially.

[15] See schematics in Appendix 2 of the second edition.

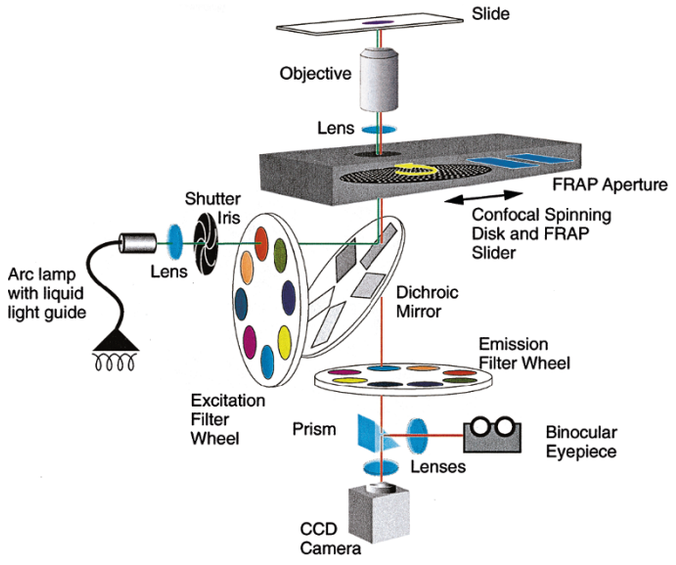

FIGURE 10.6. CARV (Atto Bioscience) disk-scanning confocal microscope. Schematic of the CARV2 optical path (BD Bioscience), a pinhole-based disk-scanning confocal system. (Image adapted from that provided by BD Bioscience.)

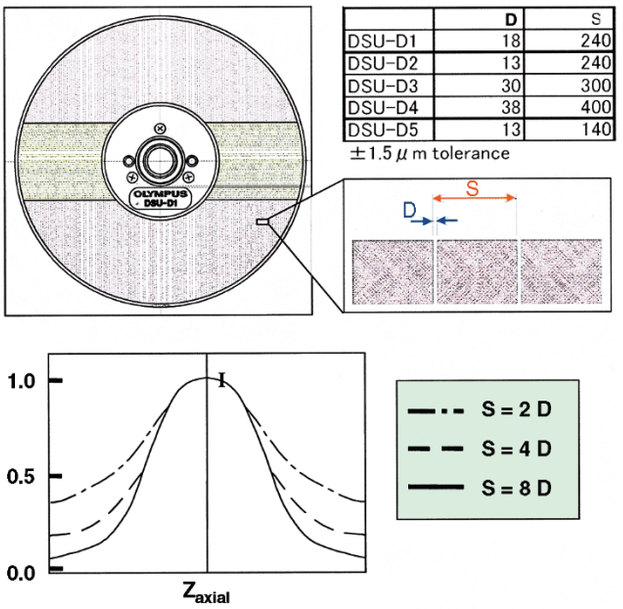

	D	S
DSU-D1	18	240
DSU-D2	13	240
DSU-D3	30	300
DSU-D4	38	400
DSU-D5	13	140

±1.5 μm tolerance

FIGURE 10.8. Characteristics of Olympus DSU slit-based confocal disk and importance of a low fill-factor for adequate axial resolution. (Top, left) Layout of the slit disk that is about the size of a CD. Approximately half the slits are horizontal (green) and half vertical (red) so that when rotated the lateral resolution is matched in the *x*- and *y*-axis. (Top, right) Blowup of a region of the disk. The slit width (*D*) and distance between slits (*S*) are indicated and a table shows the different *D* and *S* (in micrometers) of interchangeable disks. (Bottom) Plots show that axial resolution worsens as *S* decreases (for a fixed *D*) and in practice $S > 8D$ (12.5% fill factor). (Images and data adapted from those kindly provided by Olympus.)

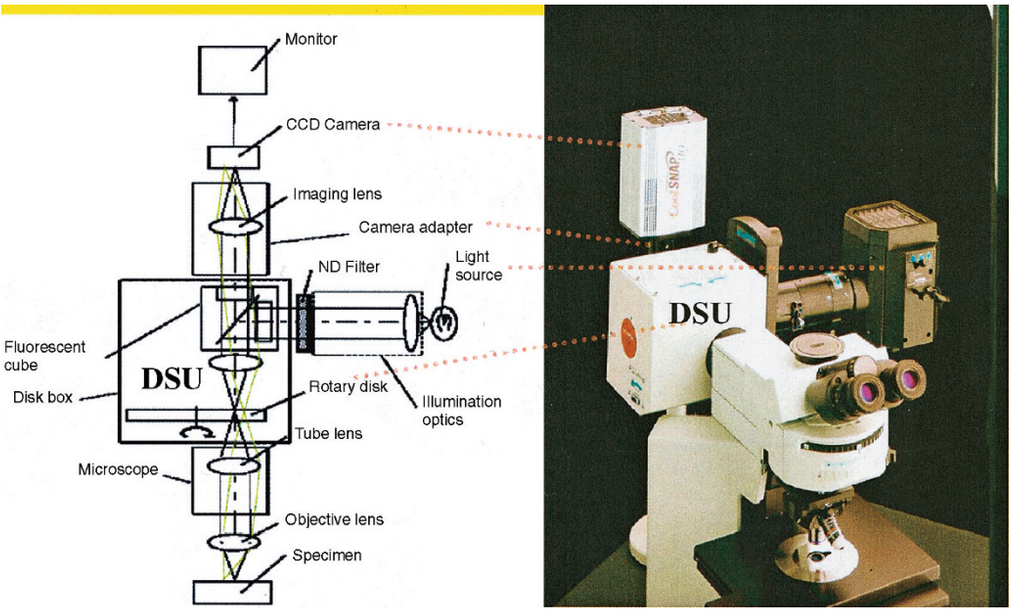

FIGURE 10.7. Olympus disk-scanning unit confocal instruments. (Left) Schematic of the optical path. (Right) Picture of the DSU (compact box) mounted on an upright microscope (can also be mounted on an inverted Olympus microscope). (Images adapted from those provided by Olympus USA.)

The Yokogawa Microlens — An Illuminating Approach

The **CSU10/22** disk-scanning head design by **Yokogawa** Electric (Japan) is an innovative twist on the single-sided disk-scanning fluorescence confocal microscope that greatly improves the excitation light budget (Fig. 10.9). Yokogawa focuses the light from a beam-expanded laser onto a disk containing **20,000 microlenses**. This disk is mounted on the same axis as the pinhole disk and in such a way that each lens focuses its light onto a different 50 µm diameter pinhole (Fig. 10.9, blue spindle). As the spacing interval between pinholes (pitch) is 250 microns, the excitation transmission would be only 4% without the microlens. With the microlens, the total **transmission through both disks is ~40%, an order of magnitude improvement** (Tanaami *et al.*, 2002). Thus, even for poorly stained samples there is adequate light.[16]

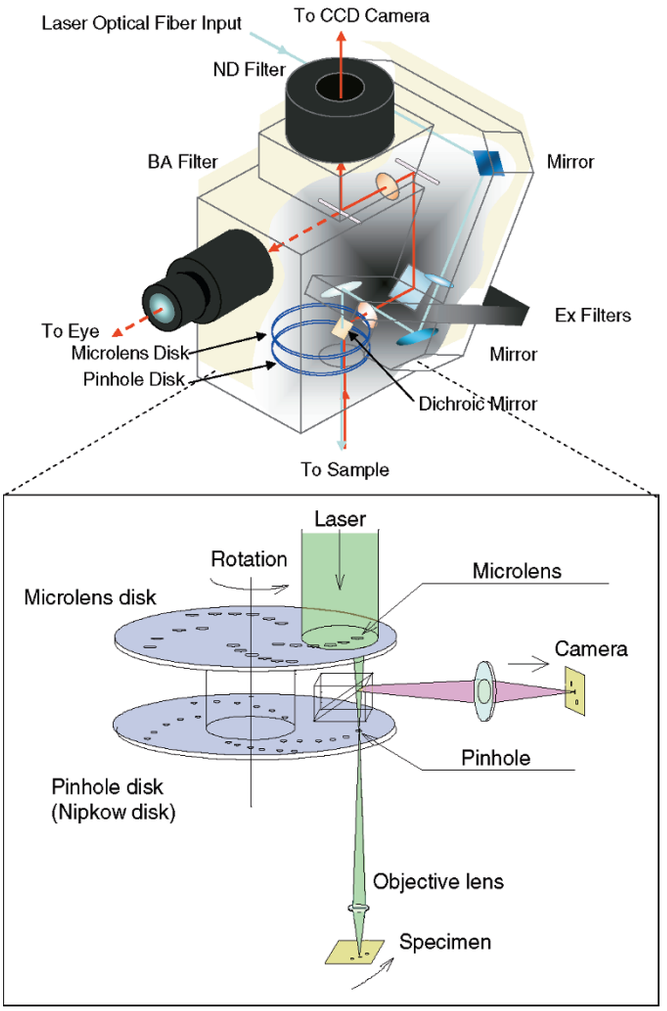

FIGURE 10.9. Schematic of Yokogawa CSU-10/22 spinning disk. Yokogawa has a microlens array top (blue disk) that focuses excitation laser light (green) onto 20,000 pinholes in a Nipkow disk located in an intermediate image plane, illuminating the sample. Emitted light (red) returns through the same pinhole and is reflected by a dichroic pellicle mirror positioned between the microlenses and the Nipkow disk and is then focused onto the camera. The positioning of the dichroic ensures that excitation light scattered by the disks is not detected. (Schematics adapted from those kindly provided by Yokogawa Electric Corporation, Japan.)

The disk rotates at 1800 to 5000 rpm, depending on the model (CSU-10 vs. CSU-21/22, respectively) and the hole pattern scans 12 frames in each rotation. This gives a theoretical maximum frame rate of 360 to 1000 fps, assuming that the camera will read out this fast and that enough signal can be produced in such a short period. In practice, operation at anything above 100 to 200 fps requires careful synchronization between the disk and the camera so that all holes move an integral number of frame crossings. Failure to do so will cause streaking in the image. Moiré effects can occur between the curved scan lines of the pinhole and the rectilinear layout of the CCD, especially at short exposure times, and this problem is worse when the CCD uses frame-transfer readout (Chong *et al.*, 2004).

At any one time ~1000 pinholes (6% of total) are illuminated. Direct viewing is possible through a monocular but laser safety concerns have eliminated this feature in some systems.[17]

A dichroic beam-splitter mounted between the two disks directs fluorescent light emerging from the pinholes to the CCD camera via a projection lens. The CSU-10 uses only a single filter cube that passes only up to three laser lines but this can be removed with some difficulty; the CSU-21/22 accommodates up to three dichroics and three emission filters but these must be installed at the factory and can not be changed. Current filters sold in the PerkinElmer version of the Yokogawa[18] system include GFP, CFP/YFP, GFP/Texas red/Cy5. Cross-talk can be an issue and thus an additional wheel of barrier filters is desirable. Several companies sell Yokogawa spinning disks units individually or as a complete package with hardware [lasers, acousto-optic modulator (AOM), cameras, *z*-piezodrivers, etc.] and software.[19]

New Fast Line Scanner — Zeiss LSM510 LIVE

Although not a disk-scanning system, the new Zeiss, LSM5 LIVE, line-scanning confocal microscope may soon emerge as a competitor to existing disk-scanning confocals. A schematic of the LSM5-LIVE is shown in Figure 10.10 and some parameters are included in Table 10.2. The largest departure from the popular point-scanning LSM510 is that the system scans a **line** of excitation over the focus plane and then detects the signal in parallel using a **1 × 512 pixel linear-array CCD**. The Gaussian beam from the laser is transformed into a plane of parallel light rays using anamorphic optics. This line of light reflects off a narrow, reflective patch in the center of an otherwise clear beam-splitter, called the Achrogate. The light sheet reflected by the Achrogate strikes a galvanometer scanning mirror located in an aperture plane, so that as it rotates, the line of light is scanned over the specimen in a direction perpendicular to its length. The objective focuses this line of light into another line, perpendicular to the first, at its focus plane. Light leaving the specimen at any angle that strikes the

[16] The total illumination power depends on the power of the laser line (e.g., 5–50 mW), its coupling efficiency to the single-mode fiber (~50%), and transmission through the beam expander, microlens, and pinhole (~40%). Light striking the 170 × 120 µm field covered by a 100× objective, should be in the range of 1–10 mW.

[17] PerkinElmer Ultraview 5-line instrument.

[18] We have extensively tested the Ultraview 5-laser line spinning disk system from PerkinElmer and, with exception of a few bugs in the file nomenclature, the hardware is well integrated and easy for new users to use. The system from Solamere offers more flexibility of setup configuration. If one integrates one's own system, attention should be paid to camera synchronization and the CSU/22 with a variable speed disk should facilitate this.

[19] Other purveyors include: Solamere Technologies, Salt Lake City, UT; Visitech, Sunderland, UK; Andor Technologies, Belfast, UK, etc.

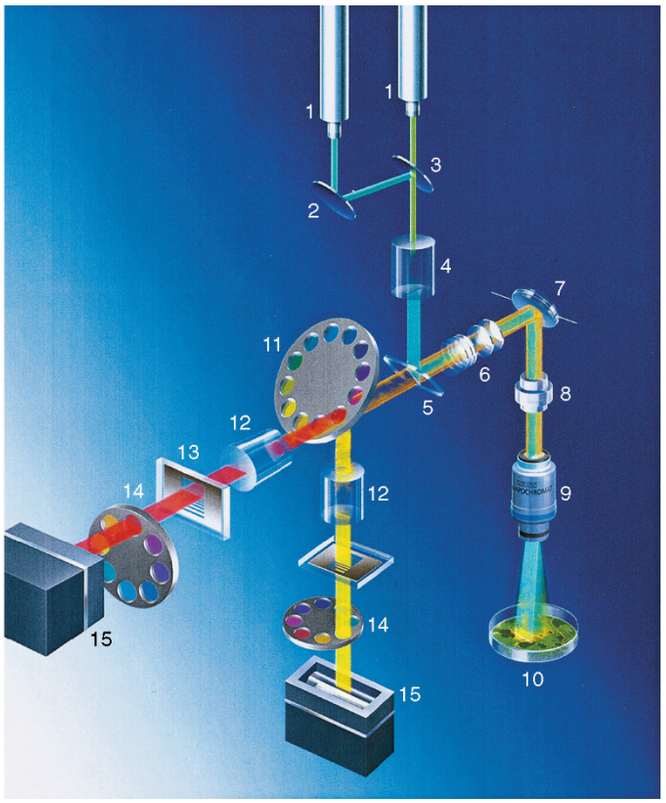

FIGURE 10.10. Schematic of Zeiss LSM5-LIVE, line-scanning confocal. 1, Laser fibers; 2–3, mirrors; 4, linear beam shaper; 5, Achrogate; 6, zoom lens; 7, scan mirror; 8, tube lens; 9, objective; 10, specimen; 11, dichroic wheel; 12, lens; 13, adjustable slit mask; 14, barrier filter; 15, linear 1 × 512 pixel, CCD. (Schematic kindly provided by Carl Zeiss Inc., Jena, DE.)

objective leaves it as a round beam, most of which does not strike the reflective patch and proceeds toward the detectors. It is then separated into two fluorescent channels by a dichroic beam-splitter and each channel passes through a "camera" lens that focuses the round beam to form an image of the illuminated line on the specimen at the surface of a glass aperture plate. The metallized reflective layer on the aperture plate is etched so as to form a number of slits having different widths. Normally, one would choose a slit having a width of 1 to 2 Airy units for the objective in use. Only the light passing the slit is transmitted to the linear CCD detector. The advantages of this system seem to be:

- Parallel illumination of 512 pixels increases the rate that data can be accumulated without reaching singlet-state saturation.
- Galvanometer scanning in a single direction increases the maximum frame rate to that set by the readout speed of the detector.
- The Achrogate reflects all the laser light, regardless of wavelength, but obstructs only about 5% of the returning signal.
- The detection slit can be adjusted independently of the illumination system to match the properties of the objective and the specimen.
- The linear CCD has a higher QE than any PMT and, if the present version is eventually replaced with an EM-CCD version (as discussed below), the noise level will be similar.

The trade-off in *xy*- and *z*-resolution is the same as for other laser-based slit-scanners. While the design is new and intriguing, more details on light efficiency and sensitivity are needed as is testing on dim fluorescent samples head-to-head with spinning disks.

NEW DETECTORS — A CRITICAL COMPONENT

A great benefit of disk-scanning confocals is their ability to produce a real-time, 2D **confocal image directly**. A PMT senses a signal that varies in time, not position, and requires a computer to assemble a viewable image. The ability to look down an eyepiece (depending on the model) and see a live image that permits you to select the best part of the specimen is a great convenience. Our eyes are exquisite detectors with an excellent dynamic range and ability to detect fine detail and motion. Although their spectral range is limited to ~400 to 600 nm and the QE is not very good (<10%), if the sample is bright enough, your eyes are the quickest way of finding a good region of the specimen.

Standard, front-illuminated **CCDs** have a QE of ~20% to 65% in the green, while with more expensive back-thinned CCD detectors, QE can approach **95%**, **far superior to a PMT**. Most standard, scientific CCDs have a 12 to 16 bit dynamic range and a noise floor of ± 5 to ± 15 electrons/pixel, depending on read speed and other design parameters. As a result, weak signals, such as those from very dim samples or single molecules, are lost in the readout noise.

A CCD camera can have good QE and still have poor noise performance; it turns photons into photoelectrons efficiently, but this signal is then obscured by the three sources of background noise: shot noise, dark charge noise, and electronic read-noise.[20] **Shot noise** is unavoidable and is due to the random Poisson statistics of collecting photons. **Dark noise** is the square root of the charge that leaks into the pixel during the exposure and depends exponentially on the CCD operating temperature (it is halved for every 8°C of cooling). **Electronic noise** increases with the capacitance (area) of the read node and the square root of the readout speed. The readout noise of a good scientific CCD is < ±10 electrons at a 1 MHz+ readout rate (see Table 10.3). This is much too high to detect single photons or the low light levels from a confocal scanner, where many pixels image voxels of the specimen contain no dye. (For more details about CCDs, see Appendix 3).

Image Intensifiers

For the last two decades, the detector of choice for fast imaging of low intensity dyes (e.g., single molecules) coupled an image intensifier with a CCD readout. In an image intensifier, photons strike a photocathode, releasing free electrons into a vacuum. Each electron is amplified usually by impact multiplication in a microchannel plate, producing a cloud of ~10^6 electrons that is then accelerated onto a phosphor layer where each one gives up its energy by producing an even larger number of photons. These photons are then conveyed to the CCD by a fiber-optics plate. The gain of the intensifier is so high that the signal in the CCD output corresponding to a single photoelectron is greater than the CCD readout noise.

The QE of an image intensifier is determined by the material used for the photocathode. The most modern cathodes use GaAsP and have an intrinsic QE of up to 30% to 40%, well into the red

[20] All detectors, including PMTs, suffer from this noise.

TABLE 10.3. Relative Parameters of CCD and EM-CCD Detectors

CCD and EM-CCD[a] Detectors	Traditional CCD: Orca ER[b]	EM-CCD: DV887BV	EM-CCD: DV860BI	EM-CCD: DV885VP
Chip: Front or back illuminated	Front	Back	Back	Front
Camera manufacturer and model	Hamamatsu (C4742-80-12AG)	Andor E2V CCD 87	Andor E2V CCD 60	Andor TI TC285
Active pixels	1344 × 1024	512 × 512	128 × 128	1000 × 1000
Pixel size[c]	6.45 µm	16 µm	24 µm	8 µm
Image area	8.67 × 6.6 mm	8.2 × 8.2 mm	3.1 × 3.1 mm	8.0 × 8.0 mm
Raw QE	70% @ 500 nm	92% @ 575 nm	92% @ 575 nm	>65% @ 600 nm
Readout speed	14.7 MHz	10, 5, 3, 1 MHz	10, 5, 3, 1 MHz	35, 27, 13, 5 MHz
Maximum cooling	–30°C	–90°C	–90°C	–90°C
Maximum EM gain (actual)	1	×1000	×1000	×1000
Dark current (minimum)	0.003 e/p/s	0.0035 e/p/s	0.004 e/p/s	0.001 e/p/s
Read noise (r.m.s.)[d]	8e @ 14.7 MHz	62e @ 10 MHz <1e with EM	60e @ 10 MHz <1e with EM	25e @ 35 MHz <1e with EM
CCD clocking	Multi-phase	Multi-phase	Multi-phase	Virtual phase
Vertical shift speed (per row)	Variable	3.4–6 µs variable	0.1–6 µs variable	0.1–6 µs variable
Maximum full frame rate	9 fps	>34 fps	>500 fps	>31 fps
Maximum frame rate (4 × 4)	>27 fps	>130 fps	>1300 fps	>100 fps
Binning	2 × 2, 4 × 4, 8 × 8	Full serial and parallel (vertical)	Full serial and parallel (vertical)	Full serial and parallel (vertical)
Fill factor	~75%	100%	100%	100%
Single pixel full well	18,000e	220,000e	200,000e	40,000e
Dynamic range of digitizer	2,250 : 1	12 bits @ 10 MHz >15 bits @ 1 MHz	12 bits @ 10 MHz >15 bits @ 1 MHz	12 bits @ 35 MHz 13 bits @ 5 MHz
A/D bit depth[e]	12 bits	14/16 bits	14/16 bits	14 bits
CCD type & mount	Progressive scan interline CCD with microlens: C-mount	Masked w/full frame transfer; C-mount	Masked w/full frame transfer; C-mount	Masked w/full frame transfer; C-mount

[a] EM-CCD cameras are sold by several companies including Andor (shown here), Hamamatsu, Roper, PCO, and others. Many use identical chips from E2V or Texas Instruments, however, other properties such as chip cooling temperature, vacuum and sealing, amplifier, hardware (e.g., TTL integration), software control and integration, internal shutters, etc., can vary considerably between manufactures and can strongly affect camera and versatility. Data kindly provided by Colin Coates at Andor Tech. (Belfast, Northern Ireland). All specifications based on manufacturers claims.
[b] This is a popular high readout speed, scientific CCD and chosen as a respective point of reference. There are hundreds of CCDs to choose from and specifications will vary considerably and are occasionally optimistic.
[c] Cameras with 18 µm pixels will require the use of a 2× phototube to produce Nyquist-sampled images with 40× and 60× high resolution objectives.
[d] Manufacture specifications; note often some of this bit depth is empty and the true dynamic range, which is determined by the ratio of the full well depth over the noise floor of the camera, is considerably smaller (e.g., if in the Orca ER 18,000e/8e = 2250, while $2^{12} = 4096$).

end of the spectrum. However, as good red performance often goes along with high dark current unless the photocathode is cooled, many intensifiers use the S-20 photocathode material commonly used in PMTs and having a QE at least 2× lower. In addition, as only about 50% of the photoelectrons reaching the micro-channel plate (MCP) are actually multiplied at all, and as the amount by which each of the remainder are actually amplified varies greatly (creating multiplicative noise), the effective QE is about half that of the photocathode itself. Finally, because both the MCP and the process of accelerating the charge onto the phosphor to make light, involve loss of spatial precision, the resolution of the entire camera is substantially less than would be indicated by the array size of the CCD.

On the other hand, the intensified CCD is the only common image sensor that can be **gated** on and off in nanoseconds,[21] permitting the extremely short acquisition bursts needed in specialty applications such as fluorescent lifetime imaging (FLIM).

Intensifier Advantages (+) and Disadvantages (–):

(+) Noise level very low; able to "see" signal from a single photoelectron.
(+) Fast gating possible.
(±) Effective QE of 10% to 25%.
(–) Pixel blooming of bright signals can occur.
(–) Scintillation or hot pixels can occur.
(–) Photocathode can be permanently damaged by brief overexposure to light.

On-Chip Electron Multiplying Charge-Coupled Device

Recently, the problem of increasing the signal from a single photoelectron above the noise level of the CCD-read amplifier has led to the perfection of on-chip **electron multiplication (EM)**. Although high-gain (10^8×), avalanche electron multiplication in a reverse-biased semiconductor photodiode has been used for some time to turn a single photoelectron into a current pulse large enough to be easily measured by electronics, efforts to apply this technique to the output of a CCD failed until recently.

The main distinction between an EM-CCD and a normal, scientific CCD is the **addition of a second horizontal register, called the gain register**, between the chip and the read amplifier (see Fig. 10.11, top). In the EM gain register, a higher voltage on one of the three sets of the charge-transfer electrodes sets up electric fields to produce, not the high gain impact multiplication found in the avalanche photodiode, but very low gain.[22] By then repeating the

[21] The camera readout time is much longer (e.g., <100 fps; Kindzelskii and Petty, 2003).

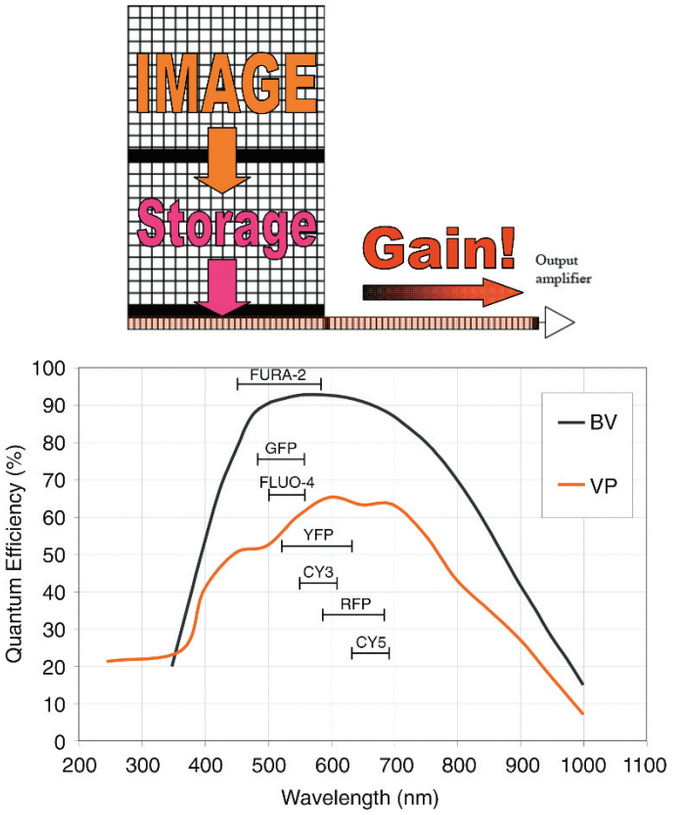

FIGURE 10.11. (Top) Anatomy of an electron multiplying CCD (EM-CCD) chip. Illumination of the imaging register (orange), read register (pink), and horizontal, readout register is to the same as any frame-transfer CCD chip. The main addition is an electron multiplying (EM) gain register (in red) before the output amplifier. (Bottom) Raw, spectral response curves of *back*-illuminated visible (*B*V) and *front*-illuminated visible (*F*V) EM-CCD chips. The emission wavelengths of some common dyes are indicated. (Data kindly provided by Colin Coates at Andor Tech.) When these chips are used with the EM register activated, the effective QE is only 50% of that shown.

process 500 or 1000 times over a line of many pixels, a gain of more than 1000 can be obtained. This makes the signal from even one photoelectron easily visible above the noise of the CCD read amplifier, even one operating at a very high read speed.[23]

With read noise effectively absent, the main remaining noise sources are dark current and clock-induced charge (CIC). Dark current can be substantially reduced by cooling the chip with a multi-stage Peltier cooler. At –80°C spurious dark current and CIC signals are reduced to about one count in 250 pixels. CIC is caused when lattice electrons are pulled into the valence band by the charge transfer process. Unmeasurable before the advent of the EM-CCD, CIC is now an important noise source that can be reduced somewhat by carefully shaping the charge transfer control pulses or made slightly worse by using back-thinned chips.

Amplifying the signal "on-chip" is appealing as it reduces the number of components and one can take advantage of the good QE of the CCD. As the signal from each pixel is amplified separately, the spatial resolution (MTF) of the EM-CCD is identical to that of the same CCD chip with the electron-multiplier turned off.

There is, of course, a price to pay and the price is increased multiplicative noise. While in a normal CCD, each photoelectron is counted the same, because of the statistical rules governing the impact ionization process in the EM-CCD, some electrons are amplified much more than others. As the noise term describing this process is of the same form as Poisson noise, and as such terms are "added" as the square root of the sum of the squares, the overall effect is to increase the "Poisson" noise level to 1.4× what it should be based on the number of photoelectrons actually produced. As the only way to reduce Poisson noise 1.4× is to count twice as many photoelectrons, it is perhaps easiest to think of the EM-CCD as having essentially no read noise but operating as though the effective QE were only 50% as high as it would be were the same CCD used without the electron multiplier. This fact must be remembered when viewing raw EM-CCD QE specifications.

Electron Multiplication Charge-Coupled Devices and Disk Scanners[24]

How do EM-CCDs improve disk-scanning confocal imaging? Good resolution and QE are important, but single-photon sensitivity means that the EM-CCD can detect very low signals when a normal CCD would only read noise. This is important not only because disk scanners without microlenses are light starved (e.g., it is like using a 95%–98% neutral density filter on your WF fluorescence system), but also because in a selectively stained specimen, by far the most common voxel intensity is zero and the EM-CCD measures zero very well.[25]

Figure 10.12 shows that even using a disk scanner and a back-thinned 90% primary QE EM-CCD, the exposure time for adequate S/N is significant (150 ms). Were a normal high quality CCD to be used instead, ~3- to 5-fold longer exposures would be needed for similar S/N. Even if one has enough light to use a normal CCD, using a more sensitive detector allows one to use less excitation and produce less photobleaching.

Currently, EM-CCD chips are manufactured by E2V (Enfield, UK) and Texas Instruments (Houston, TX) and are used in cameras from several companies: Andor, Hamamatsu, Roper, PCO, Red Shirt, and others. Several different EM-CCD chips exist and one should match the QE, pixel clock rate, pixel size, well depth, and total chip area to the biological process being investigated (see Table 10.3). For fast imaging, a smaller chip (e.g., 256 × 256 pixels) will provide increased frame rate. At present, all the available chips use full-frame transfer. While good for QE, the fact that the charge pattern moves past the image as it proceeds to the read register can cause some streaking and moiré effects with the scan lines of disk scanners even when fast vertical transfer is used (Chong *et al*., 2004). This can be avoided if EM-CCD chips incorporating interline transfer appear because such chips permit electronic shuttering at very high speed. However, unless such chips are also fitted with micro-lens arrays, these will pay a price in fill-factor and at least exhibit 2× lower effective QE.

Our tests of the Olympus DSU disk-scanning system have shown that EM-CCDs can make the difference between getting an acceptable image and seeing nothing because the signal level is below the noise threshold of our normal CCD. In addition, it

[22] The gain depends on the temperature and the exact voltage applied to a special set of charge transfer electrodes in the gain register, but is commonly about 1%/transfer, that is, a charge packet of 100 electrons would, on average, become 101 electrons after one transfer, or again on average, a single electron would become two electrons after about 100 transfers.

[23] The new chips will operate up to 35 MHz or 140 fps for a 512 × 512 array.

[24] See discussion at http://www.emccd.com.

[25] However, because of the reduction in effective QE the normal CCD begins to outperform the EM-CCD when the signal level gets much above about 100 photons/pixel. The exact crossover point depends on the read speed as this seriously changes the read noise of conventional CCDs.

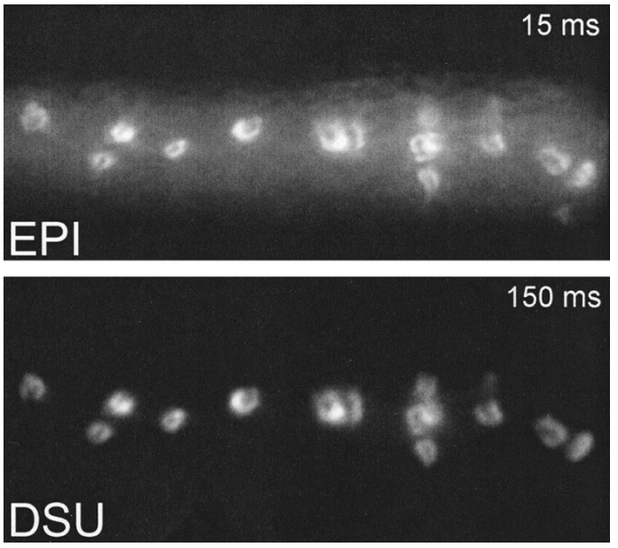

FIGURE 10.12. Disk-scanning slit confocal improves optical sectioning and S/N compared to epi-fluorescent, but requires longer exposure times. Lamprey neurons were microinjected with fluorescent-tagged phalloidin to label axons (ring-like structures). A single 15 ms exposure epi-fluorescent image was taken using an Olympus BX-51 microscope (1.1 NA 60× water-immersion objective) and an Andor 887, back-illuminated EM-CCD camera (top). After inserting the DSU disk #3 (10% transmission) a 150 ms image was acquired (same gain, bottom). In both images, the same number of photons struck the specimen. (Images kindly provided by Dr. Jennifer Morgan, Yale University Medical School.)

increased the number of high-quality images that could be acquired before photobleaching.[26]

EM-CCD Advantages (+) and Disadvantages (–):

(+) Like CCDs, EM-CCDs are photon efficient (good QE), have good contrast (MTF), are mechanically robust, and are not harmed by exposure to bright light.
(+) They have single-photon sensitivity.
(+) Ergo, they can greatly improve the speed or number of images acquired before photobleaching.
(–) No fast gating.
(–) Higher cost than normal CCD (roughly equivalent to an intensified CCD).

APPLICATIONS AND EXAMPLES OF CONFOCAL DISK-SCANNING MICROSCOPES

Comparison with Epi-Fluorescence Imaging

As discussed above, a simple disk-scanning confocal should have better optical sectioning but lower light throughput than a WF epi-fluorescence microscope. To demonstrate this we took images of the same specimen with both an epi-fluorescence setup and with an Olympus DSU spinning-slit system (10% transmission) using an Andor 512 × 512 BI EM-CCD camera. Ten times longer exposures were used with the disk in to compensate for reduced illumination striking the specimen. As seen in Figure 10.12 (processed identically), there is considerably less background fluorescence with the scanning disk in place.

Fast 3D/4D Imaging

The micro-lens–assisted spinning disks in the Yokogawa design transmit more illumination to the specimen, increasing the maximum imaging speed. Even with a traditional CCD such as the Hamamatsu Orca ER, one can record high resolution multi-color confocal stacks, as demonstrated in Figure 10.13. In ~20 s we acquired a 3D stack with 200 sections; a 3D reconstruction is shown in the lower panel. Using a single-beam confocal such as the Zeiss LSM510, acquisition of a data stack of similar size and quality would take ~5 min+. In the *xz* -views, one can see that *z*-resolution appears roughly on par with that of a good confocal LSM.

The ability to acquire confocal images rapidly allows fast 4D imaging. An example of such an application is shown in Figure 10.14 where 3D stacks of ~20 layers were each acquired in under 2.5 s and repeated over time. The scientific advantage of 4D imaging is that one gets a complete view of the process. In this example, clathrin dynamics can be seen on the upper cell surface, near the perinuclear Golgi region and also at the bottom of the cell; areas where dynamic changes occur are circled. The lower panel shows a single, 3D time point from a 4D stack of a double-labeled cell projected in space at two angles. As it is hard to convey in a static medium (this book) the visual power and the high level of biological contextual information available from looking at a 3D image over time from any angle. A movie made from this 3D data stack will be available on the Web site associated with this book http://www.springer.com/0-387-25921-X.

The challenge of how best to process and visualize large datasets will likely be an increasingly significant hurdle. It is worth commenting that while photobleaching is still a real limiting factor with a normal CCD, ultrasensitive cameras allow us to push this envelope as we enter the realm of the real-time 4D confocal imaging.

Blazingly Fast Confocal Imaging

Some biological processes can only be revealed (and understood) with high-speed imaging. Calcium sparks, flashes, and waves are examples. The 3D diffusion is so rapid that even a 1 ms exposure may not be fast enough and the process is definitely obscured in real-time (30 fps) or slower imaging.[27] Optical sectioning is needed both to improve S/N and also to sample a slice through the middle of a cell because such an image is less subject to volumetric changes in signal than is a normal epi-fluorescence image.

Maximum image acquisition speed is determined by four factors: the excitation power delivered to the sample, photophysical limits such as saturation, the disk scan speed, and the camera pixel clock and sensitivity. Because the read noise of a normal CCD rises rapidly with read speed while that of the EM-CCD does not, an ultrasensitive camera is essential. In Figure 10.15, the combination of a Yokogawa disk-scanning confocal and EM-CCD camera has permitted ~110 fps imaging of calcium sparks (top panel) or calcium waves induced by electrophysiological depolarization (bottom). These images are truly just the start of seeing life in the (ultra)fast lane.

[26] The same holds for image intensifiers, but lower QE and reduced resolution mitigate this benefit.

[27] Even current EM-CCDs may not be fast enough to fully visualize this process, as experiments with 50 ns time resolution made using a gated intensified camera (but ~30 ms repeat rates) show very fast initiation of the calcium spark (Kindzelskii and Petty, 2003).

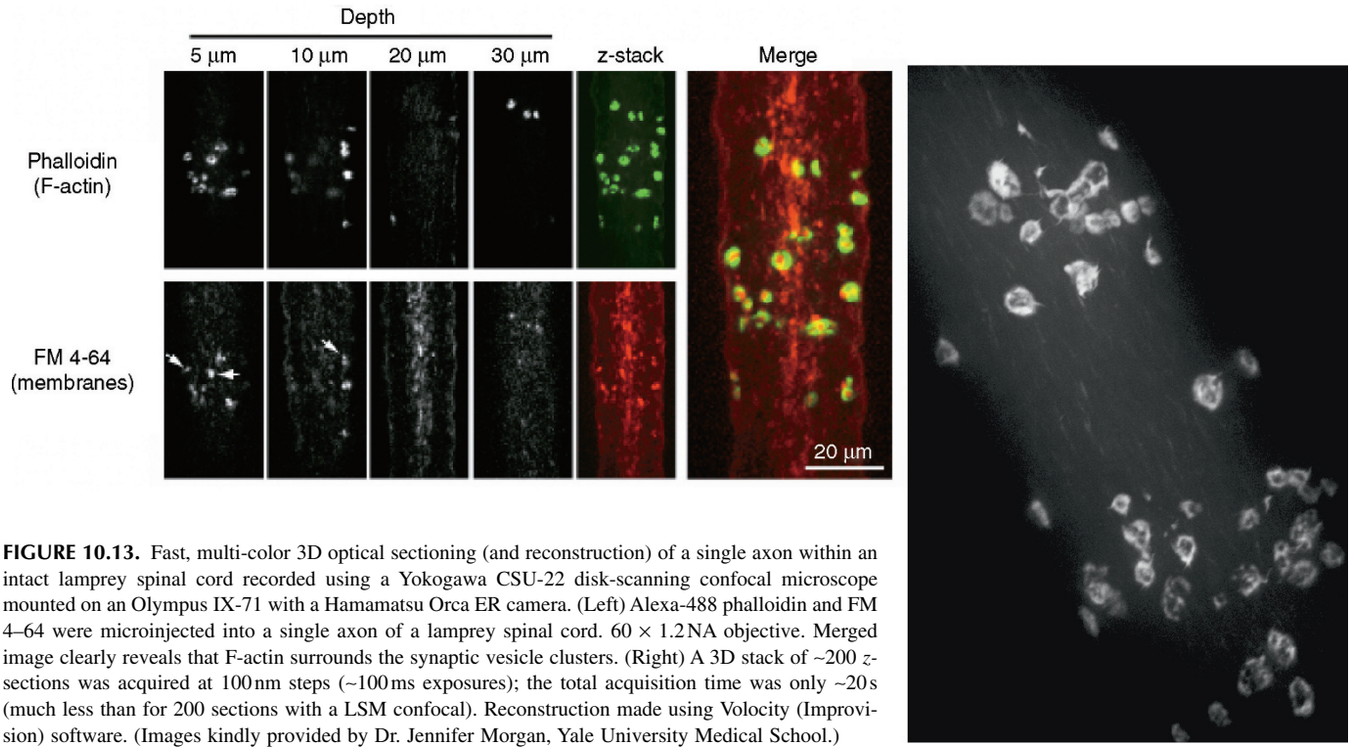

FIGURE 10.13. Fast, multi-color 3D optical sectioning (and reconstruction) of a single axon within an intact lamprey spinal cord recorded using a Yokogawa CSU-22 disk-scanning confocal microscope mounted on an Olympus IX-71 with a Hamamatsu Orca ER camera. (Left) Alexa-488 phalloidin and FM 4–64 were microinjected into a single axon of a lamprey spinal cord. 60 × 1.2 NA objective. Merged image clearly reveals that F-actin surrounds the synaptic vesicle clusters. (Right) A 3D stack of ~200 *z*-sections was acquired at 100 nm steps (~100 ms exposures); the total acquisition time was only ~20 s (much less than for 200 sections with a LSM confocal). Reconstruction made using Volocity (Improvision) software. (Images kindly provided by Dr. Jennifer Morgan, Yale University Medical School.)

FUTURE DEVELOPMENTS?

Although forecasting future development can be risky, it is always useful to consider what could be done better. One of the most challenging aspects of disk-scanning confocals is the low light budget for fluorescent excitation. The Yokogawa system avoids this at the cost of laser operation (limited wavelengths, high cost, high power/cooling. and large footprint). Two technological developments may mitigate this problem. Small, efficient **solid-state lasers** will doubtless become less expensive and even more con-

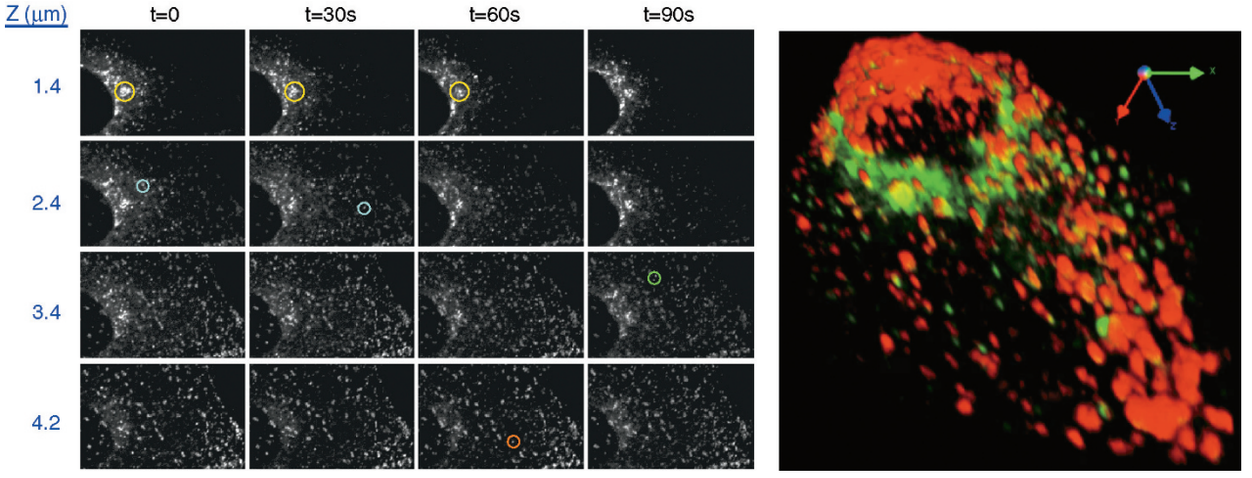

FIGURE 10.14. 3D/4D visualization of membrane trafficking with a disk-scanning confocal. (Left) 4D movie showing clathrin-GFP dynamics in PtK_2 cells imaged on an Ultraview PerkinElmer Yokogawa spinning disk system using a 60 × 1.2 NA water objective, Hamamatsu Orca ER CCD. Stacks of 21 *z*-slices were collected at 200 nm spacing, with exposure times of 100 ms/slice or <2.5 s/stack. 3D stacks were acquired at 30 s intervals. Some clathrin endosomal structures that changed over time are highlighted in different focal planes by colored circles. (Right) Living PtK_2 cells were labeled with clathrin-GFP (green) and transferrin (red) to label endosomes. A region of interest (~500 × 500 pixels × 10 slices), corresponding to 1 cell was very rapidly acquired in 4D at 1 s/stack and repeated over time (photobleaching occurred after ~50 stacks). (Images from R. Zoncu and D. Toomre, Yale University Medical School.)

venient.[28] High-intensity light-emitting diodes **(LED)** are becoming brighter and less expensive (see Chapter 6, *this volume*) and their lifespan is up to 100,000 h. In addition, they can be pulsed very rapidly, an ability that may make them useful for FLIM.

At the other end of the system, better detectors, such as microlens-equipped, interline-transfer EM-CCDs, would permit better coupling to present disk scanners. If interline-transfer chips turn out to be hard to develop, another solution to the smearing and moiré problems would be to turn off the illumination during fast vertical charge transfer. This could be implemented either by sending a blanking signal to the acousto-optical wavelength selector now used to select lines and power levels in most laser-based confocals, or by pulsing the power to an LED illumination system (see Chapter 6, *this volume*).

As camera performance improves (bigger chips, faster data transfer, better integration with system control software, etc.), new dyes are developed, and photobleaching becomes a less significant factor, HUGE amounts of data will be generated. Current cameras can read a full, 1 K × 1 chip at ~35 fps, or ~35 MB/s, or 126 GB/h! One may balk, but 4D imaging can easily require truly enormous datasets (see Chapters 32 and 50, *this volume*).

Better **data** integration, storage, visualization, and analysis are already extremely important areas that can easily become THE bottleneck in the system. More transparent data formats, such as those being used in the open microscopy environment (OME) may help.[29] This rapidly emerging problem will require companies to produce cameras that are highly integrated with acquisition, visualization, and analysis software to form a package that all works together. Both scientists and manufacturers have a vested interest here.

One may even ask the outrageous question: Will disk scanners start to replace single-beam confocals? Although it is hard to tell what will narrow the gap between disk-scanning confocals and single-beam LSMs, it should be noted that, because of their potential for high-speed imaging, CCD-equipped disk scanners are already being integrated into high content screening workstations for use in drug discovery and proteomics (outlined in Chapter 46, *this volume*).

While present disk scanners lack the ability to scan only a region of interest (ROI) to either photobleach (FRAP) or photoactivate probes, at least one manufacturer has already added a separate high-power, pulsed-laser system to a normal LSM for this purpose. There seems no reason why this could not also be done with a disk scanner.

Future disk scanners would benefit from better integration that allowed the system to make pixel-matched images using other contrast modalities such as brightfield, differential interference contrast (DIC), total internal reflection fluorescence microscopy (TIRFM), etc., and it seems quite likely that they might eventually be adapted to be sensitive to other photostates such as fluorescent lifetime and polarization. It will be of interest to many to see if this old approach to confocal imaging surges to the forefront.

SUMMARY

- Disk-scanning microscopes can produce back-scattered-light or fluorescent real-time color, confocal images.
- Disk-scanning confocals can scan 100 to 1000× faster than single-pinhole confocal LSMs.

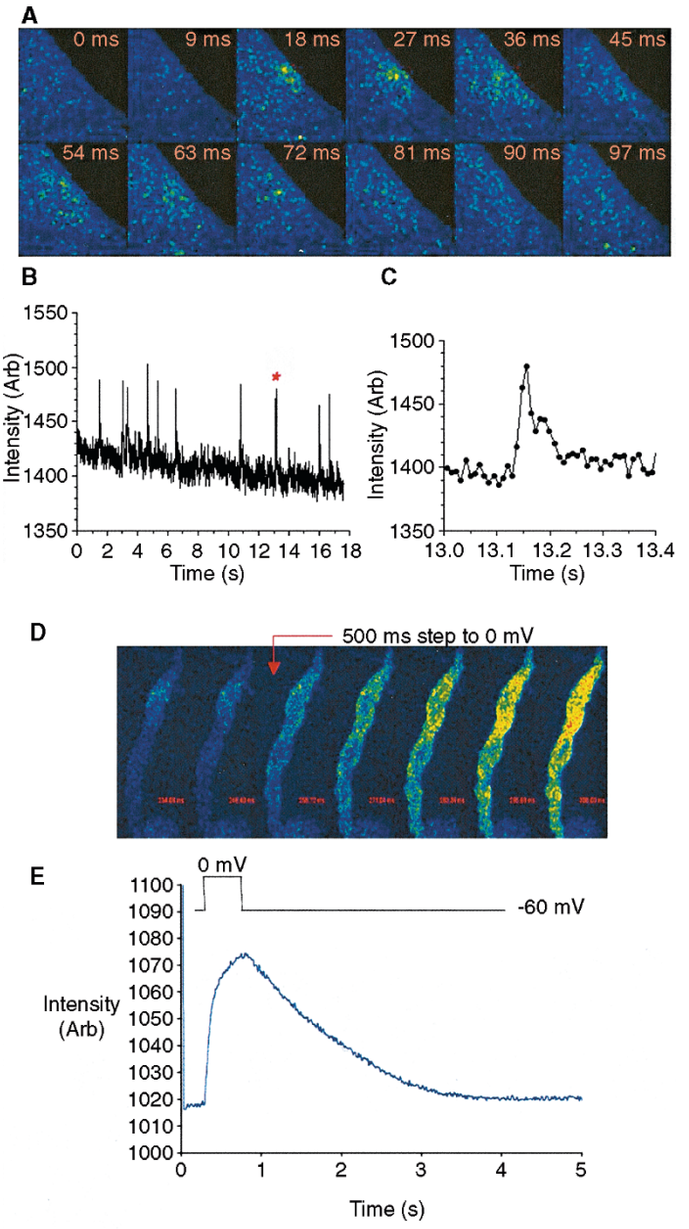

FIGURE 10.15. Very fast imaging of calcium with a Yokogawa disk-scanning confocal. (A–C) Images are from a guinea-pig bladder SMC recorded at 37°C at 113 fps (9 ms interval) on an Andor iXon camera with the 512 × 512 E2V EM-CCD (binned 2 × 2). The plots below each image show typical calcium sparks on a long timescale (B) and on an expanded timescale (C). (D, E) Images are from a rabbit urethral smooth muscle cell that was held at −60 mV and then depolarized to 0 mV for 500 ms. This experiment was recorded at 82 fps on the same camera and the montage in (D) shows false-colored consecutive images of changes in Ca^{2+} in response to the depolarization. (E) shows a record of whole cell fluorescence recorded over many seconds to demonstrate the stability of the signal and the S/N. To facilitate direct comparison with the raw video images often shown, the images, kindly provided by Dr. M. A. Hollywood, Smooth Muscle Group, Ireland (http://www.smoothmusclegroup.org), are shown magnified and unprocessed, rather than smoothed.

[28] As is evident in the Zeiss LSM5-Live slit scanner that only uses ~10 to 100 mW small solid-state lasers.
[29] http://www.openmicroscopy.org/.

- Quantum efficiency of detection can be an order of magnitude better than PMT-based LSM, reducing photobleaching and permitting the acquisition of long time series.
- Under optimum conditions, the lateral and axial resolution of a pinhole-based disk-scanning confocal is comparable to confocal LSMs. The *z*-resolution of a slit-based confocal is slightly lower.
- Pinhole/slit size must be matched to the magnification and NA of the objective lens.
- Both pinhole and slit disk designs have advantages. Compared to the disk using microlenses, the simpler slit disks are easier to interchange to properly match the slit width to the imaging conditions.
- In all cases, the fill factor of the disk limits the light throughput and, in general, greater throughput tracks with less effective optical sectioning.
- Low-noise, high QE EM-CCD cameras are critical for systems that have tight light budgets and require rapid image acquisition. Fortunately, they are now available.

As emphasized in Chapters 23, 24, and 25, image deconvolution of confocal data can be very powerful in overcoming the effects of bad imaging statistics attendant on low signal levels.

ACKNOWLEDGMENTS

Dr. G.S. Kino graciously provided many of the figures and much of the text is inspired and/or abridged from his previous versions. Olympus generously provided the DSU system for testing and Andor Tech kindly provided the EM-CCD cameras; both companies support the Yale CINEMA lab (Cellular Imaging using New Microscopy Approaches). Dr. Jennifer Morgan kindly did considerable testing with the Yokogawa and DSU cameras and provided several figures. We thank the following additional people for support and input: Dr. Charles Fangella, Dr. Chikara Abe, and Dr. Nicolas George at Olympus; Dr. Chris Calling, Dr. Colin Coates, and Dr. Mark Browne at Andor Tech.; Dr. Thomas Nicholson and Dr. Kay Mofford at PerkinElmer; Ms. Mizuho Shimizu (Yokogawa Electric Corp.); Dr. Mark A. Hollywood (Queen's University, Belfast, Ireland; Smooth Muscle Group, www.smoothmusclegroup.org); Dr. Sebastian Tille (Zeiss); Dr. Baggi Somasundaram (BD Bioscience). CINEMA lab and instrumentation are from the Ludwig Institute of Cancer Research (LICR) and a NSF-MRI instrumentation grant (DBI-0320840).

AFTERWORD

Other fast-scanning confocal designs are possible. Two instruments that are expected to come to the market soon are the "VT-infinity" instrument from Visitech (see Appendix 2) and the "LiveScan Swept Field," designed by Prairie Technologies (sold by Nikon). Both confocal heads use lasers for illumination, mirrors driven by piezoelectric elements and galvanometers to scan the sample and CCD cameras as efficient detectors. The VT-infinity system is somewhat reminiscent of the Yokogawa system in that it uses thousands of microlens and pinholes; these however are arranged as stationary arrays and scanning is achieved with galvo/piezo mirrors. The "Swept Field" system rapidly scans the sample (over 200 frames/sec) with either a slit or row of 32 pinholes (different sizes are available). In the return path a separate slit or row of pinholes is used; precise mechanical and optical alignment is likely essential for successful operation of this system. Both fast-scanning systems are intriguing in design and it will be interesting to see how they compare to spinning disk confocals counterparts.

REFERENCES

Born, M., and Wolf, E., 1980, *Principles of Optics*, 6th ed., Pergamon Press, Oxford, England.

Chong, F.K, Coates, C.G., Denvir, D.J., McHale, N., Thornbury, K., and Hollywood, M., 2004, Optimization of spinning disk confocal microscopy: Synchronization with the ultra-sensitive EMCCD, *SPIE Proc*. 5324:65.

Gaietta, G., Deerinck, T.J., Adams, S.R., Bouwer, J., Tour, O., Laird, D.W., Sosinsky, G.E., Tsien, R.Y., Ellisman, M.H., 2002, Multicolor and electron microscopic imaging of connexin trafficking, *Science* 296:503–507.

Goodman, J. W., 1968, *Introduction to Fourier Optics*, McGraw-Hill, New York.

Inoué, S., and Inoué, T., 2002, Direct-view high-speed confocal scanner: The CSU-10. Methods in Cell Biology, Vol. 70, pp. 87–127.

Kindzelskii, A.L., Petty, H.R., 2003, Intracellular calcium waves accompany neutrophil polarization, formylmethionylleucylphenylalanine stimulation, and phagocytosis: A high speed microscopy study, *J. Immunol*. 170:64–72.

Kino, G.S., 1987, *Acoustic Waves: Devices, Imaging, and Analog Signal Processing*, Prentice-Hall, New Jersey.

Kino, G.S., and Xiao, G.Q., 1990, Real-time scanning optical microscopes, In: *Scanning Optical Microscopes* (T. Wilson, ed.), Pergamon Press, Oxford, pp. 361–387.

Lichtman, J.W., Sunderland, W.J., and Wilkinson, R.S., 1989, High-resolution imaging of synaptic structure with a simple confocal microscope, *New Biologist* 1:75–82.

Lidke, D.S., Arndt-Jovin, D.J., 2004, Imaging takes a quantum leap, *Physiology (Bethesda)* 322–325.

Miyawaki, A., 2003, Fluorescence imaging of physiological activity in complex systems using GFP-based probes, *Curr. Opin. Neurobiol*. 5:591–596.

Petráň, M., Hadravsky, M., Egger, M.D., and Galambos, R., 1968, Tandem scanning reflected light microscope, *J. Opt. Soc. Am*. 58:661–664.

Petráň, M., Hadravsky, M., and Boyde, A., 1985, The tandem scanning reflected light microscope, *Scanning* 7:97–108.

Sako, Y., and Yanagida, T., 2003, Single-molecule visualization in cell biology, *Nat. Rev. Mol. Cell Biol*. Suppl:SS1–SS5.

Tanaami, T., Otsuki, S., Tomosada, N., Kosugi, Y., Shimizu, M., and Ishida, H., 2002, High-speed 1-frame/ms scanning confocal microscope with a microlens and Nipkow disks, *Appl. Opt*. 41:4704–4708.

Toomre, D., and Manstein, D.J., 2001, Lighting up the cell surface with evanescent wave microscopy, *Trends Cell Biol*. 11:298–303.

Wilson, T., 1990, Optical aspects of confocal microscopy, In *Confocal Microscopy* (T. Wilson, ed.), Pergamon Press, Oxford, 93–141.

Wilson, T., and Carlini, A.R., 1987, Size of the detector in confocal imaging systems, *Opt. Lett*. 12:227–229.

Wilson, T., and Sheppard, C.J.R., 1984, *Scanning Optical Microscopy,* Academic Press, New York.

Xiao, G.Q., and Kino, G.S., 1987, A real-time confocal scanning optical microscope, *SPIE Proc*. 809:107–113.

Xiao, G.Q., Corle, T.R., and Kino, G.S., 1988, Real-time confocal scanning optical microscope, *Appl. Phys. Lett.* 53:716–718.

Xiao, G.Q., Kino, G.S., and Masters, B.R., 1990, Observation of the rabbit cornea and lens with a new real-time confocal scanning optical microscope, *Scanning* 12:161–166.